Charles University
Faculty of Mathematics and Physics

**HABILITATION THESIS**

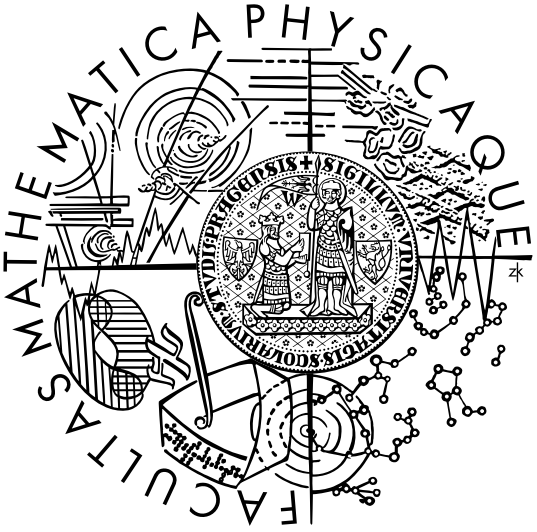


# Magnetism in UTX compounds

Jan Prokleška

Condensed Matter Physics
Prague 2021

# Contents

# Introduction

This Thesis brings together selected original results from the project "Ferromagnetic quantum criticality in clean systems", supported by the GACR agency (GA16-06422S) and solved in years 2016-2018 on the Department of Condensed Matter Physics (DCMP FMP CU) in cooperation with the Department of Magnetics and Superconductors of the Institute of Physics (Czech Academy of Sciences). The project itself was aimed at the investigation of the selected uranium and cerium ferromagnetic compounds exerted to combined extreme conditions to tune the Curie temperature to the vicinity of the absolute zero. The project was submitted in early 2015 and the idea was to investigate the so-called Quantum Phase Transitions (QTP) in clean ferromagnetic systems. Naturally, as these transitions occur at absolute zero under the change of non-thermal parameter, one can investigate only a reflection of such transition at the finite, experimentally reachable, temperatures. Within the proposal, a set of possible material families were selected, with the emphasis on the possibilities to overcome technological difficulties in the preparation of high-quality single crystal, as disorder generally was known to be one of the main adversaries in reaching the QPT.

The most fruitful group of compounds was the U$TX$ system, a system widely studied in detail earlier, due to its strong uniaxial magnetism, yet still possessing many unanswered questions. On the plus side, the technology of preparation was well known, and the DCMP excels on the worldwide level in the preparation of high-quality single crystals, necessary for the indented study. An additional advantage of this system is the presence of many members with ferromagnetic order with a relatively large span of Curie temperatures and magnitudes of ordered moments (both known to be parameters influencing the parameters of the QPT), yet with a fixed crystal structure, allowing proper disentanglement between multiple variables. On the other hand, contrary to the detailed investigation in the past decades, some of the crucial aspects of the magnetism within this group of compounds remain a mystery, e.g., in the context of the project, the unclear pattern of the pressure influence on the Curie temperature.

Our research not only indicated new compounds suitable for the investigation of QPT (with respect to the pressure evolution of the Curie temperature within the experimentally accessible range) but also shed light on the physics of both, QPT and the U$TX$ system. We show, that the small substitution may not necessarily prevent the presence of the QTP, although it may modify the character of the evolution of related properties at finite temperatures. During our investigation, we collect suitable data set allowing us to propose the correlation between the degree of the 5f-electron localization represented by the spin-fluctuation parameters (via magnetization measurement at ambient pressure only) and the response of Curie temperature on the applied pressure. One of the outcomes influences both, QPT and U$TX$ physics — we were able to show how varied technology of preparation may be the key to the acquisition of the samples with defined levels of disorder, suitable for studies of the order-disorder influence on the presence of the QTP. During the study, we obtained some in-depth information about the features of domain magnetism in the U$TX$ compounds by the measurement and analysis of the MFM images and even partially break one

of our assumptions by showing, that the magnetism within the U$TX$ group of compounds relates to different universality classes.

As the main proposer and leading scientist of the project I had an overview and significantly participated on the papers discussed in this Thesis, all of them published in the internationally recognized peer-review journals within the condensed matter physics community. The vast majority of experimental work was done within the MGML (www.mgml.eu), the open-access large research infrastructure (supported by Ministry of Education, Youth and Sport of the Czech Republic, project nos. LM2011025 and LM2018096) providing the broad scientific community unique possibilities for comprehensive experimental studies of a wide collection of physical phenomena and properties of well-defined materials in various external conditions.

The Thesis is structured as follows: Chapter 1 contains the introduction to the thermodynamics of magnetic systems, Chapter 2 gives the overview of the U$TX$ group of compounds, being the tool of the research for this Thesis. Chapter 3 is the overview of the results related to the main topic of the GACR, followed by the main result related to the general physics of the U$TX$ compounds. This Thesis is a commentary on, or more precisely a structured excerpt from the papers related to the above-mentioned topic. The full versions of these articles are collected in Appendix A.

# 1. Magnetic phase transition from the thermodynamic point of view

This chapter will review the fundamental aspects of thermodynamics related to magnetism and magnetic order, both at zero and finite temperatures.

## 1.1 Phases and phase transitions

Generally, phase transitions are transformations of a thermodynamic system from one phase (characterized by uniform physical properties with well-defined symmetry and its thermodynamic potential changes analytically for small thermodynamical variable changes) to another accompanied by an abrupt change in one or more physical properties (heat capacity, resistivity, thermal expansion, etc.) with a small change of a thermodynamical variable (typically temperature, pressure, external fields).

Phase transitions may be divided into two broad classes based on the presence of a latent heat associated with the transition.[1] During the first-order transition, the latent heat is released/absorbed leading to the observation of hysteresis.[2] The second-order (continuous) transition has no associated latent heat. During the discontinuous transitions (e.g., melting of the 3D solid, gas into liquid condensation), the two (or more) states may coexist at the transition point.

Additionally, it may show signs of hysteresis or history effects connected with the metastable nature of the original state and the macroscopically long transition times. In continuous transitions (e.g., paramagnetic-ferromagnetic transition, liquid-gas transition at the critical point, superfluid transition), the difference in energy density between the phases goes continuously to zero. Additionally, the correlation length becomes effectively infinite (critical opalescence), leading to scale invariance.

The phase transition is characterized by the change in the order parameter $\phi$ – a measure of the degree of an order across the phase transition

$$\begin{aligned} \phi = 0 \quad & \text{in the disordered phase} \\ \neq 0 \quad & \text{in the ordered phase.} \end{aligned}$$

The order parameter may have different forms and origin, depending on the nature of the underlying physics and system, i.e., scalar, complex number, vector, group element, and constructed both, in real and momentum space. The order parameter is often associated with spontaneous symmetry breaking. Nevertheless, the phase transitions can occur without spontaneous symmetry breaking (e.g.,

[1] Alternativelly, the Ehrenfest classification scheme based on the respective non-analytical derivative of the free energy (or another relevant thermodynamic potential) could be used. This scheme allows, in principle, higher-order transitions.

[2] Latent heat is typically a large amount of energy (connected with the discontinuity of the entropy across the phase boundary $L = T\Delta S$) which cannot be transferred instantaneously.

| disordered/ordered phase | order parameter | examples |
|---|---|---|
| gas/liquid | density difference | $H_2O$, He, $N_2$ |
| liquid/solid | Fourier component of density | $H_2O$, Fe |
| para-/ferro- magnetic | magnetization | Fe, Ni |
| para-/antiferro- magnetic | staggered magnetization | Cr |
| normal liquid/superfluid | superfluid density | $^4$He, $^3$He, |
| normal/super- conductor | superfluid density | Al, Pb |

Table 1.1: Illustrative examples of most common types of order/disorder transitions.

continuous crossover from liquid to gas without phase transition via supercritical fluid). Table 1.1 shows examples of order parameters in selected systems.

Quantum phase transitions (QPTs) have become an important research area of different fields of modern condensed matter physics, such as metal-to-insulator [1, 2], superconductor-to-insulator [3], superconductor-to-metal [4] and magnetic or electric order-disorder transitions [1, 5, 6, 7, 8, 9]. QPTs occur at zero temperature and can be triggered by varying a non-thermal control parameter as external pressure, chemical composition, or magnetic field and driven by a corresponding change of quantum fluctuations between phases. Among these, magnetic QPTs are of special interest, as they can have different physical origins, and their nature depends on the type of the magnetically ordered state.

While quantum critical points and quantum criticality in many itinerant and localized antiferromagnetic systems have been identified and well investigated, for ferromagnetic systems theory predicts first-order QPTs for sufficiently clean systems rather than critical points [10, 11] but available experimental evidence is somewhat limited. For weak itinerant ferromagnets, it has been shown [10, 11] that, at sufficiently low temperatures, the phase transition is generically first order with a tricritical point (TCP), which separates the line of first-order transitions at low temperatures from the line of the second-order transitions at higher temperatures. Upon applying an external magnetic field, tricritical wings appear, with their wing-tip points located at zero temperature (quantum-wing critical point, QWCP). The line of crossover temperatures $T_0$ between the TCP and the QWCP is characterized by a change of the order of the transition from first to second order.

Echoes of quantum phase transitions at finite temperatures are theoretically and experimentally challenging and unexplored topics. Particularly in metallic quantum ferromagnets, the experimental investigations are hampered by an intricate preparation of sufficiently pure samples and access to the proper coordinates in parameter space. The investigated systems are almost exclusively driven to criticality by hydrostatic pressure (see, e.g., ref. [5]), with limited use of potential probing techniques, making it difficult to distinguish between an intrinsically continuous second-order transition and an experimentally averaged and smeared out the first-order one.

| exponent | definition | condition(s) |
|---|---|---|
| $\alpha$ | heat capacity $c(t) \sim \lvert t\rvert^{-\alpha}$ | $h = 0$ |
| $\beta$ | spontaneous magnetization $m(t) \sim (-t)^{\beta}$ | $T \leq T_{\mathrm{c}},\ h = 0$ |
| $\gamma$ | magnetic susceptibility $\chi(t) \sim \lvert t\rvert^{-\gamma}$ | $h = 0$ |
| $\delta$ | critical isotherm $m(h) \sim \lvert t\rvert^{\frac{1}{\delta}}$ | $t = 0$ |
| $\nu$ | correlation length $\zeta(t) \sim \lvert t\rvert^{-\nu}$ | $h = 0$ |
| $\eta$ | correlation function $G(r) \sim \lvert t\rvert^{-d+2-\eta}$ | $t = 0,\ h = 0$ |

Table 1.2: Definition of critical exponents for magnetic systems.

## 1.2 Critical behaviour

Critical phenomena have been one of the most studied issues of physics since the critical points were discovered by Andrews [12]. The continuous (second-order) phase transitions are connected with unified behavior near and at the critical point which can be described by critical exponents. The universal behavior near critical points was described by the renormalization group theory first mentioned by Kadanoff [13] and then fully developed by Wilson [14, 15, 16]. For continuous phase transitions, the behavior close to the critical point ($T_{\mathrm{c}}$) (i.e., the critical exponents) depends only on a few parameters:

- dimensionality of the order parameter $n$
- dimensionality of the system $d$
- range of the interaction — long-range (power-law decay $r^{-n}$) vs short-range (exponential decay $\mathrm{e}^{-r/r_0}$)

Experiments show that the relevant thermodynamic variables exhibit power-law dependencies on the parameters specifying the distance (i.e., as a function of reduced temperature $t = \frac{T-T_{\mathrm{c}}}{T_{\mathrm{c}}}$) from the critical point. The definition of critical exponents for magnetic systems is listed in Table 1.2

It is desirable to investigate how a certain universal critical behavior and magnetic dimensionality are related to a given material's particularities (symmetry of crystal structure, hierarchy, and anisotropy of magnetic interactions, degree of localization of "magnetic" electrons, etc.). Large groups of isostructural compounds containing transition-element ions with one type of "magnetic" d or f electrons provide useful playgrounds for investigating these aspects. The U$TX$ compounds ($T$ = transition metal, $X$ = p-metal) crystallizing in the hexagonal ZrNiAl-type structure constitute such a suitable group of materials [17]. The crystal structure consists of U-$T$ and $T$-$X$ basal plane layers alternating along the c axis. The strong bonding of 5 f -electron orbitals within the U-$T$ layer in conjunction with strong spin-orbit interaction leads to a huge uniaxial magnetocrystalline anisotropy that locks the U magnetic moments in the c axis and thus makes these materials suitable for investigating Ising systems.

The critical magnetic behavior has so far been studied on two compounds of this isostructural group, UCoAl [18] and URhAl [19]. UCoAl is an itinerant 5 f -electron paramagnet undergoing, at low temperatures, a metamagnetic transition with a critical field of 0.7T [20]. Karube et al. [18] reported that it behaves near the critical endpoint as a 3D Ising system with short-range interactions. On

the other hand, URhAl was reported as behaving like a two-dimensional (2D) Ising ferromagnet with long-range interactions [19, 21]. The observed difference between the magnetic dimensionality of UCoAl and URhAl indicates that the layered hexagonal crystal structure and uniaxial magnetocrystalline anisotropy shared by all compounds of the U$TX$ family ($X$ = Al, Ga, Sn, In) [20, 17] is not a sufficient condition for sharing also a common magnetic universality class.

# 2. UTX group of compounds

In the U$TX$ ($T$ stands for the element from the transition metal series and $X$ stands for the element from the s–block of the periodic table) group of compounds, a large variety of magnetic properties can be found — ranging from enhanced Pauli paramagnetism in UFe$X$, spin-fluctuation behavior and metamagnetism in URu(Al,Ga) and UCoAl, respectively, to the ordering of the magnetic moments in size up to 1.5 $\mu_{\mathrm{B}}$/f.u. Most magnetic moments are found on uranium, and only small moments are observed on transition metal [22].

The reason for the variety of magnetic structures in different U$TX$ compounds is the weak interlayer exchange coupling of the U atoms and its dependence on the $T$ element (see [17] for detailed discussion). As a result, the system is susceptible to the $T$ element species, e.g., UCoGa orders ferromagnetically and UNiGa antiferromagnetically, but a small substitution of Co into UNiGa leads to the ferromagnetic ordering (see e.g. [23]). URhAl and UIrAl order ferromagnetically, UNiAl is ordering antiferromagnetically at low temperatures with a metamagnetic transition to the field forced ferromagnetic state, whereas UCoAl behaves as enhanced Pauli paramagnet with a metamagnetic transition to ferromagnetic state at low fields applied along c-axis ($B_{\mathrm{c}} \approx 0.6$T). The magnetic moment of uranium comes from the 5f electron states. Compared to 4f electron states, uranium 5f electron states are less localized (more extended) in space leading to overlapping with electron states of neighboring uranium atoms and other close atoms. The shortest distance between two uranium atoms is found in the basal plane, but transition metal atoms in the basal plane are even closer. Therefore, the 5f electron states hybridize with neighboring uranium 5f and transition metal d electron states in the basal plane, which leads to observed strong magnetocrystalline anisotropy [24, 25, 26, 27, 28].

Such an overlap together with the 5f-electron orbital moment and strong spin-orbit interaction results in an Ising-like character of the magnetism with the easy-magnetization direction along the c-axis.

Although the ground states vary across the U$TX$ system, the ferromagnetic ground state dominates [17], with varying ordering temperature and ordered moment. The advantage of such a homogeneous and extensive system of compounds is the possibility of verifying various scaling theories or, at least, using them to estimate the feasibility of such a study. Base on the theoretical works related to QPT, one can assume the proportionality between the $T_{\mathrm{TCP}}$ ($B_{\mathrm{QCP}}$) and saturated moment within one family of compounds. Additionally, many various substitutional studies within the U$TX$ system allow forming a qualified guess about the expected pressure effect on the $T_{\mathrm{C}}$, allowing to estimate the boundaries of the parameter space of interest for a given compound, or – vice versa — to look for compounds within the accessible range of given instrumentation possibilities.

For the investigation in the project following compounds were selected:

**UCo$_x$Ru$_{1-x}$Al (A.1)** is a pseudo ternary compound. Polycrystalline samples were originally prepared by Andreev et al. [29]. A ferromagnetic dome was found in doped samples with both compounds, UCoAl and URuAl being paramagnetic in the ground state. Already for 1 % of Ru, ferromagnetism is stabilized with $T_{\mathrm{C}}$= 16 K. This was confirmed on a single crystalline

sample [30, 31].

**UCoGa** orders ferromagnetically at $T_C$= 47 K [28, 20, 25]. Purwanto et al. [25] deduced magnetic moments of U atoms in the ferromagnetic state of 0.74 $\mu_B$/U. Nakotte et al. on single-crystal obtained [28] magnetic moment in the ferromagnetic state of 0.65 $\mu_B$/U. UCoGa and URhAl are isoelectronic, making the phase diagram of UCoGa interesting to compare with the URhAl one. One can estimate $T_{TCP}$ (theory predict proportionality between the $T_{TCP}$ ($B_{QCP}$) and saturated moment within one family of compounds) to roughly 10 K and the qualified guess about pressure effect on $T_C$ (based on the evolution within the substituted series [32]) places the compound to the accessible zone (rather a high temperature, hydrostatic pressure of several GPa) for direct measurement of magnetic properties allowing detailed investigation of the magnetic phase diagram.

**URhGa** was previously prepared only in polycrystalline form. Different Curie temperatures were reported. Andreyev et al. [33] reports $T_C$= 44 K and Sechovsky et al. [34] reports $T_C$= 41 K. Spontaneous magnetic moment of 1.2 $\mu_B$/f.u. was found [35]. URhGa is also isoelectronic with regards to URhAl and UCoGa. More importantly, atoms in U-$T$1 plane are the same in URhGa and URhAl, the only difference coming from the crystal structure parameter a and p-metal element. This offers an interesting possibility to compare the behavior of these two compounds.

# 3. Magnetism in the UTX compounds

## 3.1 Technological aspects (A.2)

In this Section, we will discuss the description and the effect of the magnetic domain structure on the appearance of the magnetism within a given group of compounds, in this case, the UCoGa. The clarification of the technology influences on the properties of the samples is generally essential, however in the case of quantum phase transition, where purity is the crucial factor for the observation of the first-order transition, it is of utmost importance.

We have been able to connect the technology of preparation, the presence of disorder, and the low-temperature magnetic properties in the UCoGa compound. We have prepared two single-crystalline samples, which subsequently underwent different thermal treatments. Our results document that the thermal history influences both the disorder (as indicated by the residual resistivity) and magnetism of a crystal.

The presence of the first order QPT is conditioned by sufficiently low disorder (usually crystal defects in sufficiently clean materials), however, the disorder is a property difficult to grasp experimentally, much less quantifiable exactly. Various crystal-lattice defects may be considered as the primary source of disorder. The pinning of very narrow domain walls by crystal defects has been suggested to be responsible for the large coercive fields observed in UPtAl and UIrAl single crystals [36, 37]. However, no connection to the crystal growth process nor the possible relation to the presence of crystal lattice imperfections or other types of disorder has been discussed.

Similar studies are rather seldom in the literature, usually, the variation of the thermal history is studied only with respect to the value of residual resistivity or in relation to the presence (absence, resp.) of superconductivity and magnetic ordering depending on the preparation procedure. As detailed studies are absent in the case of discussed U$TX$ compounds with ZrNiAl-type crystal structure, we generally extend our comparison to ferromagnetic uranium intermetallics. For example $UPt_3$ [38], $UGe_2$[39] and $URu_2Si_2$[40] high quality single crystals were obtained by growth by Czochralski method in tetra-arc furnace and annealing using solid-state electrotransport (SSE) method. SSE method annealing leads to efficient removal of impurities, and higher temperatures can be reached in comparison to annealing. However, due to the different evaporation rates and mobilities of elements gradient of quality/composition in the direction of current can arise [41]. High-quality single crystals of UCoGe were prepared in the tri-arc furnace, and the effect of annealing on the presence of superconductivity or magnetism was discussed[42]. In the case of our system, the effect of annealing temperature was found insignificant with respect to the quality of the resulting samples. However, in other systems, different annealing temperatures can lead to different quality of resulting material, as was shown on URhGe [39, 43], where a minimum of residual resistivity with respect to annealing temperature was reported.

| UCoGa | | $T_C$[K] | $H_c$ [T] | $\beta$ | $\varrho_0$ [$\mu\Omega$cm] | $\sigma$ [$\sigma_0$] |
|---|---|---|---|---|---|---|
| SC2A900 | annealed | 49 | 0.04 | 0.24 | 14.4 | 1 |
| SC1A800 | annealed | 48 | 0.07 | 0.22 | 19.4 | 2.7 |
| SC1A | as-grown | 48 | 0.07 | 0.25 | 18.5 | 2.7 |
| SC2A | as-grown | 48 | 0.08 | 0.24 | 44.8 | 3.54 |
| SC2C | as-grown | 44 | 0.19 | 0.33 | 75 | 21.12 |

Table 3.1: Summary of the fits of experimental data to the pinning model for soft ferro- magnets and density of defects in relation to density defects $\sigma_0$ of SC2A900 ($T_C$ – Curie temperature, $H_c$ – coercive magnetic field, $\beta$ – critical exponent for pinning constant, $\varrho_0$ – residual resistivity, $\sigma$ – density of defects).

### 3.1.1 Results

We have successfully grown two single crystals of the UCoGa compound (further denoted as SC1 and SC2). In order to achieve a controllable difference in the preparation, the rotation of the seed was turned off during the growth of SC2. From both crystals, plate-like samples were cut (perpendicular to the crystallographic c-axis). Magnetic and electrical transport measurements were done on as-grown and annealed crystals to investigate their properties and the effects of the thermal history in detail.

The results are reviewed in Table 3.1. Two pieces of SC2 (from the part of the crystal closer to the seed) were annealed for 3 weeks at 800°C and 900°C, respectively, and then cooled at a rate of 2 K/h to room temperature. As there was no difference in investigated properties between these two samples, we will only present and discuss the results obtained on the SC2A900 sample. The physical properties of the third piece of SC2 (denoted as SC2C, a piece taken from a part of the crystal located far from seed and close to the melt) have not been influenced by the additional annealing process, too. Based on results obtained from annealing SC2, we chose to anneal SC1 samples for three weeks at 800 °C (SC1 A800) to prevent possible interactions with the tantalum foil. In all cases, the annealing does not lead to any observable changes to the crystallinity or composition of the samples, at least as observed within the resolution of the used methods.

From the low-temperature magnetization curves, we can evaluate the evolution of coercive fields ($H_c$) – the lowest $H_c$ value was observed for the annealed sample SC2A900, whereas the as-grown SC2C shows the highest coercive field. The as-grown SC1A crystal exhibits an $H_c$ value comparable to that reported in literature [28]. The temperature evolution of the magnetization curves shows the exponential decrease of $H_c$ with increasing temperature for all investigated crystals, similarly to soft ferromagnets [44]. The coercive field is proportional to domain wall pinning factor $k$ [45], which is exponentially dependent on temperature [44]

$$k(T) = k(0)\mathrm{e}^{-\frac{T}{\beta T_C}}$$

where $T_C$ is Curie temperature, and $\beta$ is the critical exponent for pinning constant.

Results of the fits within the pinning model for soft ferromagnets are given in Table 3.1. The different $H_c$ values corresponding to different samples can be attributed to the different densities of defects reflecting different thermal histories of

the samples (defects acting as pinning centers and preventing smooth movement of domain walls). It has been shown that the coercive field is proportional to the square root of the density of defects and that it also depends on the domain wall area [46]. Since our single crystals are of nearly the same chemical composition and ordering temperatures, sample invariable values of the exchange and magnetic anisotropic energy in all samples may be expected, resulting in comparable domain-wall areas in all our samples. Consequently, we can determine the relative change in the density of defects taking the SC2A900 sample as a reference with the lowest coercive field (see Table 3.1).

As a probe of material quality (related to the lattice defects), we used the residual electrical resistivity $\varrho_0$, reflecting the scattering of conduction electrons on defects and other lattice imperfections. The temperature dependences of electrical resistivity of all studied samples are qualitatively comparable, the notable exception is the SC2C sample with the resistivity dominated by the large residual resistivity in the entire temperature range (the residual resistivity ratio RRR = R(100 K)/R (2 K) = 1.8), contrary to all other samples (RRR = 6.3–11.4) and the effect of magnetic ordering on the character of the temperature dependence is negligible.

The high degree of disorder in the SC2C sample is also reflected in a considerably reduced $T_C$ value compared to all the other samples. The observed $\varrho_0$ values for all samples are also shown in Table 3.1. There we can see that the lowest residual resistivity and coercive force were obtained for the SC2A900 sample, whereas the highest values refer to SC2C.

### 3.1.2 Discussion

The considerable difference in quality between the as-grown SC1 and SC2 crystals can be attributed to different parameters of the growth procedure. In contrast to the SC1 crystal rotation, the SC2 crystal was not rotating during the growth that probably caused a less optimized solidification process in the latter case, presumably causing a higher concentration of defects.

Annealing at 900°C, which is just a few degrees below the melting temperature, significantly improved the quality of the SC2A single crystal to the levels fully comparable with optimally grown SC1, as documented by both the observed magnetization and electrical resistivity behavior. The SC2C sample represents an exceptional case where the lattice damage was severe and probably new local thermal equilibrium has been reached, which could not be influenced by annealing. This is also seen in the change of critical exponent $\beta$, which differs from other crystals. If we compare the residual resistivity of the SC2A900 sample with those available in the literature of other members of the U$TX$ family with the ZrNiAl crystal structure, we see that the best values are of the order of 10 $\mu\Omega$cm (URhAl [47], UCoAl [48, 49], UNiGa [50]). These values are fully comparable to the best values obtained in the current study.

High coercive-field values related to domain-wall pinning have been reported in other U$TX\tilde{\text{f}}$erromagnets from the ZrNiAl family (UPtAl, UIrAl). The authors reported the residual resistivity values of single crystals of UPtAl $\varrho_0 = 68$ $\mu\Omega$cm [36] and UIrAl $\varrho_0 = 87$ $\mu\Omega$cm [51]. No annealing treatment has been mentioned, however. Nevertheless, the reported high $\varrho_0$ values corroborate the scenario that the

crystal defects were the primary source of the reported high coercive fields similar to our case.

## 3.2 Magnetic domain walls structure (A.3)

Magnetocrystalline anisotropy (MA) is manifested by locking the macroscopic magnetic moment in a particular direction of a crystal, the easy magnetization axis (easy axis). The strength of MA is characterized by a magnetic field (anisotropy field $H_a$), which needs to be applied in the perpendicular direction (hard axis) to rotate the moment from the easy axis to the hard axis.

When cooled in a zero magnetic field, the bulk of a ferromagnetic (FM) material decomposes into mutually antiparallel FM domains (except flux closure domains) to minimize the magnetostatic energy. Neighboring domains are separated by domain walls of a thickness determined by the balance between the anisotropy energy[1] $E_a$ and the exchange-interaction (EI) energy ($E_{ex}$). The EI favors a slow rotation of the magnetization, while the MA prefers a sudden magnetization reversal. In the 3d-electron ferromagnets with a typically weak MA and strong EI ($E_{ex} \gg E_a$) the domain-wall thickness may be even hundreds of distance between nearest magnetic ions. On the other hand, the strong MA ($E_a \gg E_{ex}$) in f-electron ferromagnets may cause a reduction of the domain wall width down to a few interatomic distances [52, 53].

The direct imaging and investigation of domain structures in U compounds have been done on polycrystalline samples at room temperature (RT) in materials with a high concentration of 3d transition metals [54, 55] with magnetic moments which are ferromagnetically coupled by strong EI resulting in high $T_C$-values ($\gg$RT). The only report on the single crystalline material containing uranium has been recently published [56] on the $UMn_2Ge_2$. Although this material has comparable [57] anisotropy (roughly ¼) in comparison to the compound under study [24], the formation of magnetic domains is determined by the ordering of Mn moment at higher (above RT) temperatures.

This section summarizes the direct low-temperature investigation of a domain structure in a U 5f-electron moment ferromagnet with $T_C \ll$RT.

### 3.2.1 Results and discussion

In the case of a ferromagnet with strong uniaxial anisotropy, a domain pattern created by domain branching can be observed at a surface perpendicular to the easy axis [58]. The evolution of magnetic domains during the magnetization process in UCoGa was studied at 20 K (in the ordered state) through magnetic force microscopy (MFM). In the zero-field-cooled (ZFC) state, one can see a labyrinth-like domain structure. At 0.01 T, a very similar domain pattern is observed. Domains magnetized in the same direction as the probe expands with further increasing magnetic field. For $\mu_0 H = 0.1$ and 0.3 T, the domains disappear consistently with the reaching of the saturation of magnetization. New domains appear with decreasing field for $\mu_0 H < 0.05$ T when the sample becomes demagnetized from

[1] The anisotropy energy $E_a$ is equal to the energy difference between the magnetic moment directed along the hard and the easy axis.

the saturated state. These domains have a different shape than those observed in the ZFC state. Nevertheless, some of them are pinned to the same surface point where a lattice defect can be expected. The lattice defects, which serve as centers of pinning of the magnetic domain walls, are usually unaffected by the applied magnetic field and are fixed in the lattice in the magnetization/demagnetization process. An analogous magnetization process was observed in a negative applied magnetic field.

The temperature evolution of magnetic domains upon ZFC cooling completes the picture. The clear development of magnetic domains just below $T_C$ is observed. The contrast increases upon cooling as expected for increasing magnetic moments of the individual domains. A gradually developing domain-branching pattern is observed upon cooling from 40 K to lower temperatures. The shape of the domains at the surface changes only slightly, with decreasing temperature emphasizing the morphological details. The width of the surface domains $W_s$ decreases with temperature decrease, reflecting the narrowing of the magnetic domains inside the sample with increasing magnetic moment.

The domain-wall energy $\gamma_W$ in a ferromagnet with a strong uniaxial anisotropy can be calculated by using the equation

$$\gamma_W = \frac{W_s m_s^2}{49\mu_0}$$

where $m_s$ is the spontaneous magnetization and $\mu_0$ the permeability of vacuum [58, 59, 60]. A $\gamma_W$ value of 1.1 mJ/m$^2$ is obtained with the $W_s$ and $m_s$ values, determined at the lowest temperature of measurement (5 K) where the thermal effects are minimized.

Although most FM materials are characterized by Bloch domain walls, a simple calculation shows that this is not the case for UCoGa. The width of a Bloch domain wall in UCoGa can be calculated from the equation

$$\delta = \frac{\gamma_W}{K_1}$$

where $K_1$ is the anisotropy constant [61]. Using the value $K_1 = 88$MJ/m$^3$ [24] and the above given domain-wall energy of 1.1 mJ/m$^2$, a Bloch domain wall thickness $\delta = 12.5$pm is obtained. This value is about 30 times smaller than the distance between the two nearest magnetic U ions (350 pm [62]) in UCoGa. The failure of the Bloch-domain-wall model is not surprising. In this model, the magnetic moment rotates between neighboring magnetic ions by an angle of about 1° in case of weak MA and/or strong EI, which is typical for the 3d-electron ferromagnets. In contrast, in the case of UCoGa and most U 5f-electron ferromagnets, the MA is very strong while EI is relatively weak.

The critical exponents suggest (see Section 3.5) that UCoGa belongs to the universality class of the 2D Ising system with long-range magnetic order [63]. As the crystal structure of UCoGa is characterized by a distorted kagome lattice of U ions, we can derive the EI energy from $T_C$ using the relation for the 2D Ising ferromagnet kagome lattice [64]. The smallest element of a domain wall in UCoGa is a trio of U ions forming an equilateral triangle with two U ions with parallel moments and one U ion with an antiparallel moment. The EI energy such a trio of moments is equal to $k_B T_C \frac{\ln\left(3+2\sqrt{3}\right)}{2}$ and when divided by the area of the

smallest element of a domain wall, it leads to $\gamma_W = 1.4 mJ/m^2$. This value is in reasonable agreement with the value of 1.1 $mJ/m^2$ determined above from the surface domain width.

We can conclude that UCoGa exhibits a typical surface-domain structure for a strongly anisotropic uniaxial ferromagnet, consistent with the huge uniaxial MA observed in this compound. The MFM images show the appearance/disappearance of magnetic domains during the magnetization/demagnetization processes with increasing/decreasing applied magnetic field. In the partially magnetized state, the magnetic domain walls are pinned to lattice defects which have been identified in the AFM and MFM images. Analysis of available data leads to the conclusion that the high energy of the uniaxial magnetocrystalline energy assisted by the relatively low energy of ferromagnetic exchange interaction in UCoGa causes that the domain walls are extremely narrow, equal to the distance between the nearest magnetic U neighbor ions with antiparallel magnetic moments in the U-$T1$ basal plane of the hexagonal structure.

Analogously, the same unique domain-wall properties are expected for other uniaxial U ferromagnets, characterized by high anisotropy energy in combination with moderate values of the exchange energy.

## 3.3 Pressure as an external parameter (A.4, A.5)

This section will discuss two examples of pressure evolution within the U$TX$ family — UCoGa and URhGa compounds. The work was focused on probing the expected ferromagnet-to-paramagnet quantum phase transition induced by high pressure and on the general features of the $p-T(-H)$ phase diagram. Comparing these two compounds is of at most interest, as they are both members of a homogeneous family of compounds, or more precisely – assumed to be homogeneous enough, where the majority of studied compounds show the monotonous suppression of the magnetic ordering temperature with applied hydrostatic pressure. Rather surprisingly, the URhGa was found to be the second known compound within this family, showing the increase of the Curie temperature under applied hydrostatic pressure (the only previously known sole exception is UPtAl where a similar increase Curie temperature has been observed in low pressures [65]).

### 3.3.1 UCoGa

At ambient pressure, UCoGa exhibits collinear ferromagnetic ordering of uranium magnetic moments $\mu_U \approx 0.74\mu_B$ (at 2 K) aligned along the c-axis of the hexagonal crystal structure below Curie temperature $T_C = 48$K.

For the high-pressure measurements, small pieces of larger crystal have been selected with residual resistivity $\varrho_0 \approx 10\mu\Omega$cm, which can be classified as clean within the given family of compounds [5]. With applied pressure, a clear decrease of the $T_C$ is visible, accompanied by smearing out of the $T_C$ - related anomaly at higher pressures. For a better understanding of pressure evolution, the power-law fit ($\varrho = \varrho_0 + AT^n$) at low temperatures is used for description. At low pressures, the resistivity exponent is close to 2, in agreement with the ferromagnetic ground state of the compound. With increasing pressure, the abrupt

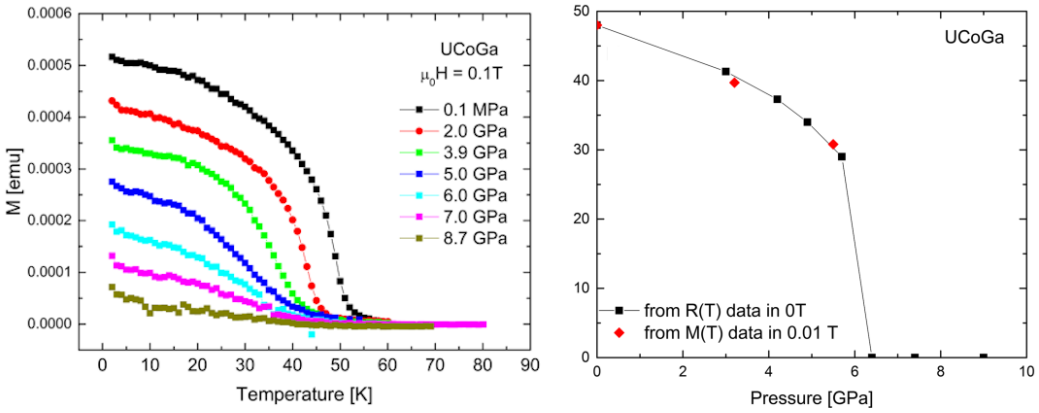


Figure 3.1: Left: The temperature dependence of magnetization as measured in 0.1T field applied along the c-axis for various applied pressures. Right: Pressure dependence of the ordering temperature determined from the measurements of temperature dependence of magnetization and electrical resistivity.

change of the evolution in the vicinity of 6 GPa indicates the order-disorder transition. The resistivity exponent drops close to ⅝ at the presumed quantum phase transition as expected by the theory of 3D spin fluctuations [66]. Similar values were observed in the isostructural URhAl [67] and UCoAl [68] compounds in the vicinity of the suppression of long-range ferromagnetism, indicating the importance of spin fluctuations in the magnetism of this family of compounds. This is in accordance with the increase of residual resistivity at higher pressures in a non-magnetic state due to the additional scattering on disordered magnetic moments. The pressure evolution of magnetic properties was measured directly to confirm the sudden suppression of magnetism and loss of long-range ordering. The temperature dependence of the magnetization measured at 0.1T (field cooled) demonstrates well-defined $T_C$ value at low pressures, being suppressed to 30 K at 6 GPa (see Fig. 3.1). With increasing pressure, the saturated magnetization at 2K shows continuous suppression to about ⅔ of ambient value, followed by a rapid drop in the vicinity of critical pressure.

From the obtained results, the magnetic phase diagram can be constructed (see Fig. 3.1). Both transport and magnetic measurements reveal continuous suppression of transition temperature down to 30 K at 6 GPa, which we identify as the tricritical point (TCP), followed by rapid change of observed quantities (both on transport and magnetic properties) related to the loss of long-range magnetic ordering. The phase diagram follows the expectations for the clean itinerant ferromagnet (see e.g. [5]), i.e., continuous suppression of ordering with increasing pressure down to TCP, where the rapid drop in observables is expected in accordance with the presence of the first-order transition. Similar behavior was observed in URhAl [67] and UCoAl [69]. The presented experimental data are in agreement with comparable literature data and theoretical predictions [5]. The temperature of the TCP is rather high as compared to similar compound URhAl, nevertheless, the sample used in study [67] has significantly higher residual resistivity (65$\mu\Omega$cm) and the URhAl has a lower magnetic moment. From theory, it is known that both increase of disorder (reflected in higher residual resistivity) and smaller magnetic moment affect the tricritical temperature negatively [70].

### 3.3.2 URhGa

Up to our study, the URhGa compound has been characterized only at ambient pressure and in polycrystalline/powder form. We prepare the single crystal, compare its properties to previously published data and study the evolution of magnetism under pressure, comparing it to the neighboring UCoGa (see section above) and discuss the peculiar behavior in the context of the entire U$TX$ series.

The measurement of heat capacity at ambient pressure shows a clear transition at $T_C = 41$K being quickly suppressed by applied magnetic field along the c-axis. The magnetization study at low temperatures revealed a ferromagnetic ground state with the ordered moment of $1.1\mu_B$/f.u. for field applied along the c-axis.

The parameters mentioned above lead us to the conclusion, that the compound qualify as a suitable candidate for the possible search of scaling laws close the ferromagnetic quantum criticality [5] with UCoGa compound being the benchmark partner (same structure and magnetic order, similar ordering temperatures, nevertheless half ordered moment, cf. previous subsection). In order to test this scenario, a pressure study has been made. With increasing pressure, the transition remains visible on the thermomagnetic curves at low fields (0.01T), however, it can be clearly seen that contrary to expectation, the Curie temperature increases with increasing pressure and reaches the plateau in the range of 5-8 GPa. As the temperature dependencies indicate and field scans at low temperatures confirm, the ground state becomes more robust (in the sense of increased coercive field). On the other hand, the saturated moment is partially reduced ($-0.05\mu_B$/f.u./GPa).

The obtained results reveal a continuous increase of transition temperature up to 48 K in 6 GPa, followed by a plateau up to the highest pressure used in this study ($\approx 8.5$GPa). This behavior is rather rare in the studied isostructural U$TX$ family of compounds as the majority of published pressure studies report monotonous suppression of the ordering temperatures down to the presumable quantum phase transition. The sole exception is UPtAl, where a similar increase in Curie temperature has been observed in low pressures [65]. The reasoning for such behavior will be discussed in Sec. 3.6 in detail.

## 3.4 Pressure and substitution interchangeability (A.6, A.7)

This Section discusses the possibility to tune a specific system at easily accessible conditions to the vicinity of its quantum phase transition. The physics is demonstrated on Ru-doped UCoAl, driven by pressure or substitution to and across the tricritical point and follows the first-order transition line to the theoretically presumed quantum phase transition. These findings open the possibilities for further in-depth studies of classical and quantum critical phenomena at easily reachable conditions.

We have chosen UCoAl, whose ground state is paramagnetic at ambient pressure and zero magnetic field but located in the immediate proximity to the TCP and close to a ferromagnetic instability, and thus is very sensitive to a magnetic field, pressure, and alloying [17, 71, 72, 69, 48]. UCoAl is, therefore, an excellent candidate for such studies compared to related U$TX$ compounds, where the

QPT may be hidden in the superconducting dome (URhGe [73], UCoGe [74]) or accessible with extreme difficulties (URhAl [67]). In the case of UCoAl, the QPT is expected to be positioned at small negative hydrostatic pressures and it is known that the ferromagnetic ground state can be achieved by doping with a small amount of transition metal. However, the substitutional tuning is known to introduce disorder, causing the suppression of TCP and thereby leading to a continuous transition to the lowest temperatures [5]. In order to clarify the presence of the QPT and investigate the vicinity of the TCP, we prepared high-quality single-crystalline samples of UCoAl with sub percent doping by Ru of 0.5 and 1% to avoid the effect of disorder.

Here we show that the $UCo_{1-x}Ru_xAl$ system can be driven to and across the QPT by weak Ru doping or by hydrostatic pressure, and we were able to resolve the details of the phase diagram in the vicinity of the TCP and the presence of a regime where long-range ferromagnetism and paramagnetism coexist due to the first-order transition below TCP. The results are fully consistent with theoretical predictions and offer the possibilities for further in-depth studies of quantum critical phenomena at easily achievable conditions.

As we mentioned above, the undoped compound UCoAl is paramagnetic at ambient pressure and zero magnetic field but located in the immediate proximity to the TCP and close to a ferromagnetic instability. Like all the members of the family, it exhibits a strong magnetic anisotropy [17] accompanied by an Ising-like character of the magnetism with the easy-magnetization direction along the c-axis.

The effect of Ru doping on the magnetic behavior of UCoAl is best seen in the temperature dependence of the low-field magnetization and the magnetization curves at selected temperatures, all measured for fields applied along the c-axis of the single-crystal samples. In the sample doped with 0.5% of Ru, a shift of the metamagnetic transition at the respective temperatures to lower fields is observed, in comparison to the pure UCoAl ($H_c \approx 0.7$T) whereas the spin-fluctuation maximum [75] in the low-field M vs. T dependence is preserved (see Fig. 1). This indicates the presence of strong spin fluctuations associated with the metamagnetic behavior similar to that in pure UCoAl.

In contrast to the behavior of $UCo_{0.995}Ru_{0.005}Al$, $UCo_{0.990}Ru_{0.010}Al$ behaves as a ferromagnet with a Curie temperature of 16 K. Here, we observe neither a sign of a local maximum in the temperature dependence of the magnetic susceptibility nor metamagnetic behavior. Thus the two doped samples probe different magnetic regions of the phase diagram close to the TCP and thereby allows one to explore the change of nature of the magnetic state by tuning the system towards and across the QPT.

We first discuss the magnetic state of $UCo_{0.995}Ru_{0.005}Al$ sample. The hysteresis at the metamagnetic transition vanishes in the 9 K magnetization loop, allowing the determination of the crossover point at 0.3T to be 9 K. However, at low temperatures, a finite remnant magnetization emerges, indicating ferromagnetic ordering. The remnant magnetization decays exponentially with temperature showing a tendency to saturation at low temperatures. Indeed, measurements at low temperatures ($T < 2$ K) unveil the fully developed ferromagnetic loop below 0.6 K). At 1.8 K, the coercive field of the ferromagnetic loop and the critical field of the metamagnetic transition are comparable, and the two phenomena cannot

be distinguished. The zero-field cooled and field-cooled curves at 5 mT indicate ferromagnetic order in the vicinity of 4 K.

This allows us to conclude that the compound exhibits a ferromagnetic ground state, yet metamagnetism (a feature intimately connected to the paramagnetic ground state of UCoAl) exists close to and above the Curie temperature. This indicates the presence of or close proximity of the sample to the tricriticality in the generalized phase diagram.

To elucidate our findings that indicate the coexistence of ferromagnetism and paramagnetism in the limited range of parameter space of 0.5% Ru-substitution, we have investigated the evolution of the ferromagnetic state of the sample doped with 1% Ru under pressure – in other words, tuning the ferromagnetic sample towards and across the expected QPT.

At low pressures (up to 0.2 GPa), the ground state remains ferromagnetic, yet the Curie temperature is quickly suppressed with a rate of 25 K/GPa. With further increase of pressure, the change (decrease) of the Curie temperature levels off at 0.26 GPa and 7 K. Simultaneously, one observes an additional curvature in the low-temperature magnetization (close to the coercive field), which becomes more pronounced at higher pressure or temperature. Schematically, one can capture the evolution of the magnetic state with pressure by plotting the basic characteristics of the metamagnetism and by adding the coercive field of the ferromagnetic part of the magnetization loop. The resulting Fig. 3.2 clearly shows the main features of the magnetic states developing with pressure. It can be seen that the temperature evolution of the coercive field (ferromagnetic quantifier) remains intact at these modest pressures, in agreement with the negligible pressure dependence of the Curie temperature. In contrast, the critical field of the metamagnetic transition (paramagnetic-ground-state quantifier) monotonously evolves. An estimation of the evolution of the critical field with respect to pressure gives 2.5 T/GPa, being comparable to the value reported for pure UCoAl [72]. 14 This can be described as the presence of phase separation within a limited window of pressures, composed of an itinerant ferromagnet phase and a metamagnetic phase with identical characteristic and pressure-independent temperatures $T_{\mathrm{C}} = T_0 = T_{\mathrm{tr}} \approx 7$ K. With further increasing pressure, ferromagnetism is quickly suppressed and a purely paramagnetic ground state exists. The behavior is illustrated in Fig. 3.2 in which one can see the complementarity in the evolution of the remnant magnetization (related to the ferromagnetism) and the magnetization step at the metamagnetic transition (related to the paramagnetic part of the ground state). Based on the presented data, we locate the TCP for $UCo_{0.990}Ru_{0.010}Al$ at 0.2 GPa and 8 K.

In order to investigate the critical behavior across the above-described loss of long-range ferromagnetism, we have investigated the electrical resistivity under hydrostatic pressures as well. The obtained temperature dependencies were evaluated assuming the $\varrho = \varrho_0 + AT^n$ behavior.

For the $UCo_{0.990}Ru_{0.010}Al$ sample, at low pressures and low temperatures (in the ferromagnetic ordered state), the resistivity follows a $T^2$ law as expected from the Fermi-liquid theory (see Fig. 3.2). With increasing pressure, the characteristics abruptly change most notably, the power drops to ³⁄₂.

Comparing our results to those for pure UCoAl we observe a similar value of the $A$-coefficient but different exponent $n$. While the electrical resistivity of pure UCoAl behaves [76] as $T^{\frac{5}{3}}$, both our samples behaves as $T^{\frac{3}{2}}$. Recently Kirk-

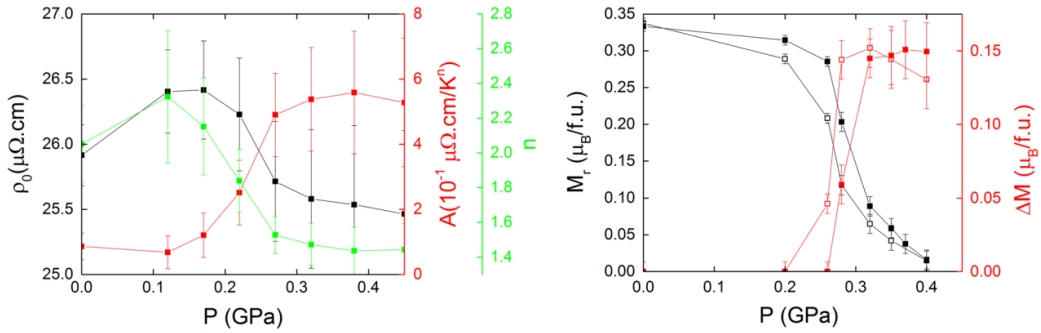


Figure 3.2: The evolution of transport and magnetic properties across the presumable QPT for the $UCo_{0.990}Ru_{0.010}Al$ sample. The error bars indicate the uncertainties of derived quantities. Left: The pressure dependence of residual resistivity ($\varrho_0$), $A$ coefficient and power $n$ as evaluated from the temperature dependencies of the electrical resistivity. Right: Pressure dependence of the magnetization step $\Delta M$ at the metamagnetic transition and remnant magnetization $M_r$ at two selected temperatures.

patrick and Belitz [77] explained $T^{\frac{3}{2}}$ behavior by the existence of static droplets of ordered phase in magnetically disordered phase. Applying the proposed scenario leads us to the conclusion that although the UCoAl at ambient pressure and $UCo_{0.990}Ru_{0.010}Al$ under applied hydrostatic pressure have the same magnetic ground state [29], the microscopic nature of this state is different, and reflects the paths necessary to reach such a state. In the case of UCoAl, the compound has a well-ordered crystal structure, and its electronic configuration places it on the verge of magnetism resulting in an archetypal metamagnet. On the other hand, the substituted sample, even forced to the same state, reflects its history with the irregularities in the lattice acting as a condensation nuclei leading to the survival of the nFl behavior (reminiscence of TCP) across the extended range in the parameter space. With respect to this result, a detailed study comparing the pure UCoAl and doped samples at even higher pressures is desirable. Interestingly $UCo_{0.995}Ru_{0.005}Al$ exhibits the minimum at the same temperature as $UCo_{0.990}Ru_{0.010}Al$ (Fig. 5) in pressures between 0.12 GPa and 0.38 GPa. This is in agreement with $UCo_{0.995}Ru_{0.005}Al$ being in the mixed-phase part of the phase diagram.

### 3.4.1 Discussion

The presented experimental data are fairly consistent with the theoretically proposed general phase diagram for itinerant ferromagnets [10, 11] describing the suppression of ferromagnetism as a function of external parameters (pressure, composition, see Fig. 3.3). Starting from the well-defined ferromagnetic behavior (1% Ru doping in this study), phase separation is observed between TCP and QPT both by 0.5% Ru doping at ambient pressure and 1% Ru doping at hydrostatic pressures between 0.26 and 0.40 GPa. This strongly supports the existence of the expected first-order transition between TCP and QPT.

The presented experimental evidence can be established in several directions. First, we have shown that a very small amount of substitution may not lead to

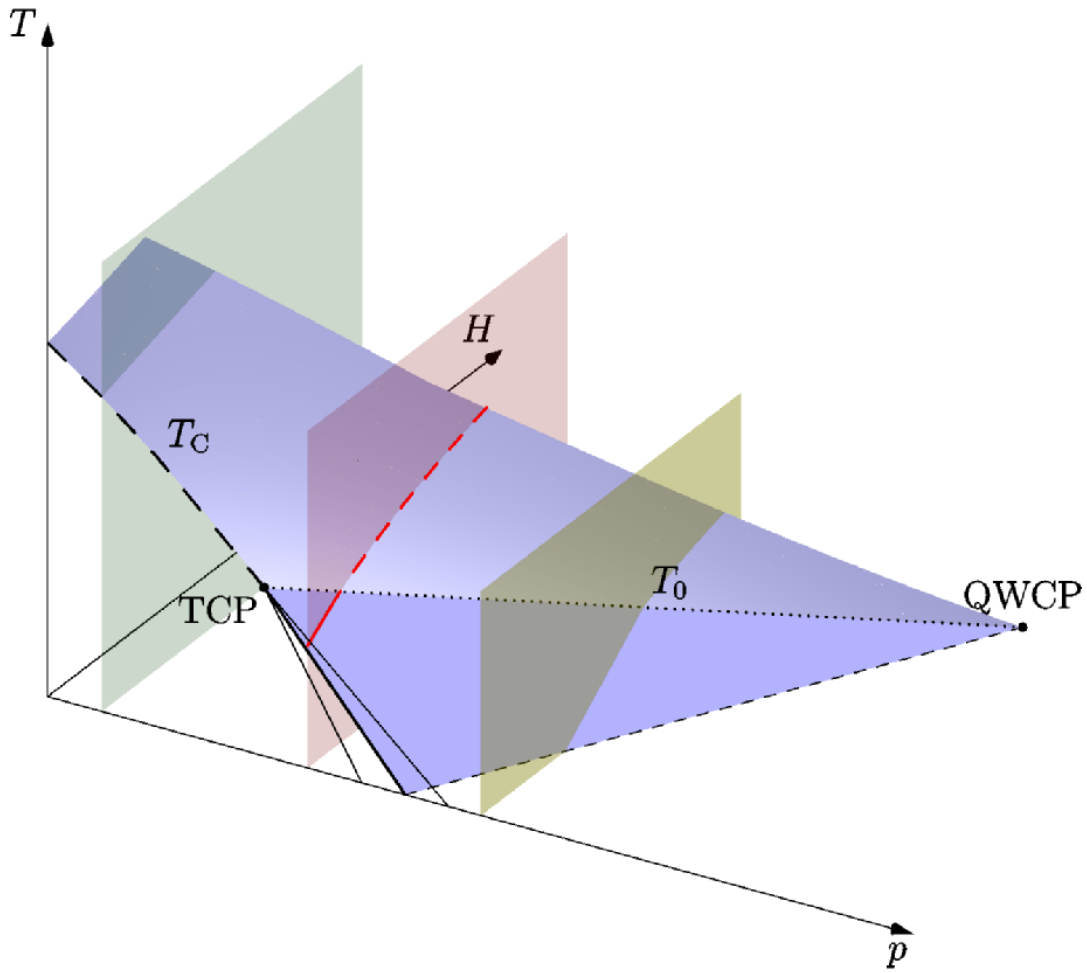


Figure 3.3: Schematic view of the proposed phase diagram near the tricritical point (TCP) in the temperature ($T$)-—magnetic field ($H$)-—control parameter ($p$) space based on the experimental data. Within the presented study, the control parameter is either hydrostatic pressure or substitution. Starting at high temperatures and H = 0, the second-order transition is indicated by a dashed line, spreading to a non-zero field as the second-order transition plane (light blue surface). Below TCP ($H = 0$, solid line) and crossover temperature $T_0$ for $H \neq 0$ (dark blue) the transition becomes first-order accompanied by the presence of hysteresis (for simplicity indicated only for $H = 0$). Planes for fixed $p$ indicate position of samples used in this study—green ($UCo_{0.990}Ru_{0.010}Al$), red ($UCo_{0.995}Ru_{0.005}Al$) and brown (UCoAl). The red line indicates the phase transition line ($\mu_0 H_c$) for the $UCo_{0.995}Ru_{0.005}Al$, indicating both first-order (solid) and second-order (dashed) transition. For simplicity, the phase boundaries are sketched only for non-negative fields.

suppression of the first-order transition and consequently the presence of a TCP in the phase diagram but is sufficient for tuning the system towards (and across) the QPT. This opens new possibilities for the investigation of QPT in metallic ferromagnets and related phenomena. This would suggest a possible way to design and prepare in a controlled way a single-crystalline material having the QPT at ambient pressure, unscreened by superconductivity, for in-depth studies of related finite-temperature phenomena.

Second, the experimental possibility of smooth passing of the TCP and interchangeability of pressure and composition variations allows us to make a rough estimation of the critical field of the wing-tip QCP. Following basic thermodynamic considerations within the mean-field model [10], we obtain a value of about 6 T, which is in good agreement with earlier pressure studies on pure UCoAl [72] and roughly one-half of the values reported in recent experimental studies [48].

Third, our experimental data show the importance of the proper and complete investigation of reflections of quantum critical phenomena. The system under investigation (small Ru doping of UCoAl) clearly shows the $n = 3/2$ power law in resistivity at low temperatures in paramagnetic ground state, being characteristic for pure transition metal-based systems (e.g., archetypal MnSi [9] or $ZrZn_2$ [78]). This behavior is not fully understood in these systems, and probably different mechanisms may be responsible. In the case of small Ru-doping or off-stoichiometric U(Co,Al), one sees the same paramagnetic ground states as in pure UCoAl, however, the temperature dependence of resistivity may reflect subtle changes in the electron-electron and electron-phonon correlations leading to the striking difference of the transport properties with respect to those of pure U$TX$ compounds, deserving detailed investigations both on a theoretical and experimental level. Within this context, it should be noted that although the strongly anisotropic U$TX$ (see for e.g., discussion on spin fluctuation anisotropy in ref. [71]) may follow [79] the general features of the magnetic phase diagram [10, 11] the exact microscopic mechanism behind the non-analytical corrections to the Fermi liquid theory remains unknown.

Finally, the possibility of crossing the TCP employing pressure or composition allows one to perform a detailed investigation of the basic thermodynamics related to phase separation in the immediate proximity of the QPT. This is of particular importance, since contrary to expectations based on thermodynamic considerations, it is known that phase separation in some quantum ferromagnets and other systems can occur away from the coexistence curve of a first-order phase transition [77].

## 3.5 Universality classes (A.8)

Magnetization isotherms of single crystals of three hexagonal U$TX$ ferromagnets UCoGa [20, 27, 26, 28], URhGa [80, 81, 35], and $UCo_{0.98}Ru_{0.02}Al$ (a close analog of $UCo_{0.990}Ru_{0.010}Al$ discussed in previous sections, for an overview of U(Co,Ru)Al system, see [29]) were measured at temperatures in the vicinity of their Curie temperature to investigate the critical behavior near the ferromagnetic phase transition. These compounds adopt the layered hexagonal ZrNiAl-type structure and exhibit huge uniaxial magnetocrystalline anisotropy. The critical $\beta$, $\gamma$ and $\delta$ exponents were determined by analyzing Arrott-Noakes plots [82, 83], Kouvel-Fischer plots [84], critical isotherms, scaling theory [85], and Widom scaling relations [86]. The values obtained for URhGa and UCoGa can be explained by the results of the renormalization group theory for a two-dimensional (2D) Ising system with long-range interactions similar to URhAl reported by other investigators. On the other hand, the critical exponents determined for $UCo_{0.98}Ru_{0.02}Al$ are characteristic of a three-dimensional (3D) Ising ferromagnet with short-range interactions suggested in previous studies also for the itinerant 5f-electron paramagnet UCoAl situated near a ferromagnetic transition. The change from the 2D to the 3D Ising system is related to the gradual delocalization of 5f-electrons in the series of the URhGa, URhAl, and UCoGa to $UCo_{0.98}Ru_{0.02}Al$ and UCoAl compounds and appears close to the strongly itinerant nonmagnetic limit. This indicates possible new phenomena that may be induced by the change of dimensionality in the vicinity of the quantum critical point.

Our results show that there is a clear distinction between the magnetism in the studied compounds, the values of critical exponents, and other relevant information obtained on URhGa, UCoGa, and $UCo_{0.98}Ru_{0.02}Al$ single crystals are displayed in Table 3.2. The information available in the literature for UCoAl [18] is included for comparison and further discussion.

The critical exponents of URhGa and UCoGa can be explained similarly to the URhAl case [18] by introducing a weak long-range magnetic exchange interaction in the form $J(r) \sim r^{-(d+\sigma)}$), where $\sigma$ is the range of the exchange interaction [87]. Fischer et al. [87] applied the renormalization group theory for a system with an interaction $J(r)$ for which the equation for the approximation of $\gamma$ has been obtained in the form

$$\gamma = 1 + \frac{4}{d}\left(\frac{n+2}{n+8}\right)\left(\sigma - \frac{d}{2}\right) + \frac{4}{d}\left(\frac{n+2}{n+8}\right)\frac{2}{d}\left(\frac{n-4}{n+8}\right)\left(1 + \frac{2\left(3 - \frac{1}{4}\left(\frac{d}{2}\right)^2\right)(7n+20)}{(n-4)(n+8)}\right)\left(\sigma - \frac{d}{2}\right)^2 \quad (3.1)$$

The value of $\sigma$ ranges from $d/2$ to $d$, for $\sigma \geq d$, behavior typical for short-range interactions is expected, and for $\sigma \leq d/2$, behavior is described by mean-field theory.

The obtained values of $\gamma$ were examined using Eq. 3.1 by substituting the possible values of $d$ (dimension of the system) = 1, 2, or 3 and $n$ (dimension of the order parameter) = 1, 2, or 3 in all possible combinations and comparing the resulting values of $\sigma$ for $\gamma$ and $\beta$. The best agreement for both URhGa and UCoGa has been found for the 2D Ising system with long-range (LR) interactions,

| | $\beta$ | $\gamma$ | $\delta$ |
|---|---|---|---|
| URhGa | 0.41 | 1.19 | 3.89 |
| LR 2D Ising ($\sigma = 1.21$) | 0.39 | 1.18 | 4.03 |
| UCoGa | 0.37 | 1.26 | 4.32 |
| LR 2D Ising ($\sigma = 1.28$) | 0.36 | 1.26 | 4.5 |
| $UCo_{0.98}Ru_{0.02}Al$ | 0.33 | 1.24 | 4.92 |
| 3D Ising | 0.33 | 1.24 | 4.79 |
| UCoAl | 0.26 | 1.2 | 5.4 |

Table 3.2: Critical exponents obtained by the analysis of experimental data, critical exponents for respective models, and for UCoAl [18] for comparison.

similar to URhAl [19]. The resulting $\sigma$ value and corresponding $\beta$, $\gamma$, and $\delta$ values are listed in Table 3.2 and Fig 3.4 with values for URhAl [19] and 3D Ising, 3D XY, 3D Heisenberg, 2D Ising, and mean-field models.

On the other hand, we have confirmed that $UCo_{0.98}Ru_{0.02}Al$ behaves like a 3D Ising system with respective values of critical coefficients. The 3D Ising behavior of $UCo_{0.98}Ru_{0.02}Al$ resembles the behavior of pure UCoAl reported by Karube et al. [18].

The 5f-electrons in U intermetallics are known to have a dual character (partially localized, partially itinerant) [88, 89, 90]. The localized and itinerant characters appear in different proportions depending on crystallographic and chemical environments of the U ion being reflected in a wide range of their magnetic behavior. This is a consequence of the wide extension of the 5f-wave functions, which allows for considerable direct overlaps between 5f-wave functions of the nearest-neighbor U ions and hybridization of valence electron states of ligands (5f-ligand hybridization). As a result, the original atomic character of the 5f-wave functions is destroyed while the related magnetic moments are washed out and adequately reduced. In the strong 5f-5f overlap and 5f-ligand hybridization limits, the 5f-electrons are predominantly itinerant, the 5f magnetic moments vanish, and the magnetic order is lost (UCoAl in our case). Rhodes and Wohlfarth [91] and Wohlfarth [92] proposed that the ratio $\frac{\mu_{\mathrm{eff}}}{\mu_{\mathrm{s}}}$ between the effective and spontaneous magnetic moments can be taken as a measure of the degree of itinerancy of the magnetic electrons. In Table 3.3, we can see that $\frac{\mu_{\mathrm{eff}}}{\mu_{\mathrm{s}}}$ increases along the series as listed from top to bottom. In the Rhodes-Wohlfarth scenario,

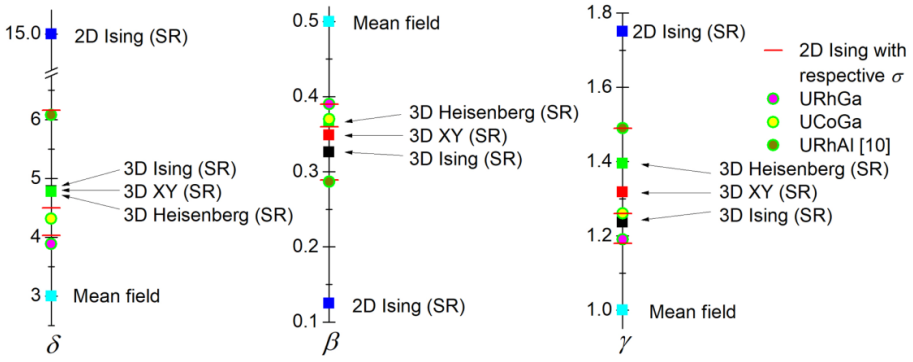


Figure 3.4: Obtained critical exponents for URhGa and UCoGa in comparison to URhAl [19] and values of three-dimensional (3D) Ising, 3D XY, 3D Heisenberg, two-dimensional Ising, and mean field models.

| | $\mu_{\mathrm{eff}}$ $\frac{\mu_{\mathrm{B}}}{\mathrm{f.u.}}$ | $\mu_{\mathrm{s}}$ $\frac{\mu_{\mathrm{B}}}{\mathrm{f.u.}}$ | $\frac{\mu_{\mathrm{eff}}}{\mu_{\mathrm{s}}}$ | Univers. class | $a$ [pm] | $c$ [pm] | |
|---|---|---|---|---|---|---|---|
| URhGa | 2.45 | 1.17 | 2.11 | 2D Ising | 700.6 | 394.5 | [93] |
| URhAl | 2.5 | 1.05 | 2.38 | 2D Ising | 696.5 | 401.9 | [19, 93] |
| UCoGa | 2.4 | 0.65 | 3.69 | 2D Ising | 669.3 | 393.3 | [28, 93] |
| $UCo_{0.98}Ru_{0.02}Al$ | 1.73 | 0.36 | 4.81 | 3D Ising | 669.1 | 396.6 | |
| UCoAl | 1.6 | 0.3 | 5.33 | 3D Ising | 668.6 | 396.6 | [94, 20] |

Table 3.3: The values of effective and spontaneous magnetic moment, $\mu_{\mathrm{eff}}$ and $\mu_{\mathrm{s}}$ , respectively, and the $\frac{\mu_{\mathrm{eff}}}{\mu_{\mathrm{s}}}$ ratio and lattice parameters for our studied URhGa, UCoGa, and $UCo_{0.98}Ru_{0.02}Al$ compounds completed by the values for URhAl and UCoAl. The $\mu_{\mathrm{s}}$ value for UCoAl is the magnetic moment in the field just above the metamagnetic transition. The true $\mu_{\mathrm{s}}$ value for UCoAl is indeed equal to 0; the ground state is paramagnetic.

the degree of itinerancy of 5f electrons increases when proceeding from URhGa toward UCoAl.

Further inspection of Table 3.3 reveals that the change from 2D Ising to 3D Ising universality class happens when the 5f electrons become considerably itinerant due to the reduction of $a$ parameter, connected with the decreasing U-U and U-$T$ interatomic distances within the basal plane. This agrees with Takahashi's [95] description, in which for more itinerant systems, larger anisotropy is needed to suppress the region of 3D behavior than more localized systems. This explains the 3D behavior of UCoAl and $UCo_{0.98}Ru_{0.02}Al$ even though the magnetocrystalline anisotropy is comparable to that in URhGa, UCoGa, and URhAl [17, 20, 28, 96]. Also, we see that the p-metal affects the degree of localization/itineracy, which affects the universality class of the system. The hierarchy of exchange interactions will undoubtedly play an essential role in controlling dimensionality.

## 3.6 Relation between spin fluctuation and pressure evolution (A.9)

Nowadays, ferromagnetic quantum criticality is a heavily studied phenomenon. Hydrostatic pressure acting on the studied material has proven to be a suitable parameter for tuning magnetic state.

In this Thesis, we focus on a group of compounds from the U$TX$ family having the hexagonal ZrNiAl structure. Many of these compounds are ferromagnetic with a relatively large span of Curie temperatures and magnitudes of ordered moments [17] and, as discussed in detail earlier, may be used to study discontinuous phase transitions with variable parameters of magnetic order, yet with a fixed crystal structure. In several of these compounds, the presence of a discontinuous phase transition has been recently confirmed (see detailed discussion in Section 3.3). On the other hand, two members of this group, UPtAl [97] and URhGa (see Sec. 3.3.2), respectively, show an initial (in the range of several GPa) increase of $T_{\mathrm{C}}$ with increasing pressure. This leaves an open question about the possibility of predicting the pressure behavior of $T_{\mathrm{C}}$ in these compounds.

In this Section, Takahashi's spin-fluctuation theory (TSFT) [98] is used to determine if an increasing $T_C$ with increasing pressure can be expected. In this theory, the total amplitude of the local spin fluctuations (SF) is constant as a function of temperature. This enables one to determine the value of $F_1$ , the mode-mode coupling term as the coefficient of the $M^4$ term in the Landau expansion of the free energy

$$F(M) = F(0) + \frac{1}{2(g\mu_B)^2\chi}M^2 + \frac{F_1}{4(g\mu_B)^4 N_A}M^4$$

and the values of $T_0$ and $T_A$ represent the distribution widths of the SF spectrum in energy and wave-vector space, respectively.

The compounds targeted by the study are UCoGa, with $T_C = 48$K [27, 81] and $T_C$ decreasing with applied pressure (see Section 3.3.1), and URhGa with $T_C = 41$K [81] and $T_C$ increasing with pressures up to 6 GPa (Section 3.3.2). The analysis of magnetization data observed at ambient pressure reveals a clear difference of the corresponding $F_1$, $T_0$, $T_A$, and $T_C/T_0$ values obtained for the two $UTX$ compounds. A considerably higher degree of 5 f -electron localization (higher $T_C/T_0$) in conjunction with the narrower SF spectrum both in energy and wave-vector space (smaller $T_0$ and $T_A$) have been documented for URhGa in comparison with UCoGa. The results of the analysis of pressure-induced changes of the above mentioned TSFT parameters corroborate the proposed scenario of $\frac{dT_C}{dp} > 0$ for URhGa in contrast to $\frac{dT_C}{dp} < 0$ for UCoGa. The evolution of $\frac{dT_C}{dp}$ of the hexagonal $UTX$ ferromagnets with the ZrNiAl-type structure including UCoGa and URhGa reveals correlation with $T_C/T_0$ ratio across this isostructural series. The corresponding data known for orthorhombic $UTX$ ferromagnets and $UGe_2$ indicates that the above correlation does not have universal validity for all U ferromagnets.

The values of Curie temperature were estimated as the temperature of the inflection point of thermomagnetic curves measured in a low applied field (0.1 T) at various pressures. For UCoGa, $T_C$ decreases while for URhGa $T_C$ increases with increasing pressure, as discussed earlier.

The magnetization isotherms of UCoGa and URhGa were measured at 1.8 K, at the same pressures as the corresponding temperature dependencies of thermomagnetic curves. The values of spontaneous magnetization ($M_s$) were obtained by extrapolating the parts (above 1 T in order to avoid effects related to domains) of magnetization curves to zero magnetic field. The $M_s$ values obtained for UCoGa and URhGa at different pressures are listed in Table 3.4. In UCoGa, $M_s$ is clearly decreasing with increasing pressure, whereas the $M_s$ of URhGa decreases only slightly between 0 and 0.6 GPa, and remains unchanged with higher pressures up to 1 GPa.

The Arrot plots of UCoGa and URhGa magnetization data were evaluated at different pressure points in order to determine $M_s$ and $T_C$, and the TSFT parameters $F_1$, $T_0$, $T_A$, and $T_C/T_0$, Table 3.4.

To facilitate the discussion of these parameters and their development with pressure, the complexity of the role of U 5f-electrons on the electronic structure and magnetism should be taken into account. The variable dual character of the 5f-electrons of U ions (partially localized, partially itinerant) [88, 89, 90] found in various crystallographic and chemical environments in U compounds is

| | $p$ [GPa] | $T_C$ [K] | $M_s$ [$\mu_B$/f.u.] | $F_1$ [K] | $T_A$ [K] | $T_0$ [K] | $T_C/T_0$ |
|---|---|---|---|---|---|---|---|
| UCoGa | 0 | 48.8 | 0.56 | 3060 | 1750 | 267 | 0.182 |
| | 0.73 | 46 | 0.53 | 2320 | 1700 | 330 | 0.139 |
| | 1 | 44.5 | 0.5 | 1880 | 1720 | 424 | 0.105 |
| URhGa | 0 | 41.1 | 1.17 | 741 | 480 | 83 | 0.495 |
| | 0.6 | 42.2 | 1.16 | 776 | 498 | 85 | 0.496 |
| | 0.86 | 42.6 | 1.16 | 824 | 508 | 83 | 0.512 |
| | 1.12 | 42.8 | 1.16 | 853 | 513 | 82 | 0.521 |

Table 3.4: Experimental values of $T_C$ and $M_s$ with calculated values of $F_1$, $T_A$, $T_A$, and $T_C/T_0$ from TSFT for UCoGa and URhGa at different pressures.

reflected in the wide range of their observed magnetic behaviors. UCoGa and URhGa were selected for our study because they represent two groups of U$TX$ compounds characterized by different signs of pressure effect on $T_C$, quantitatively expressed by $\frac{d \ln T_C}{dp}$ (see Table 3.4). The two compounds have similar values of Curie temperature ($T_C = 48.8$ and 41.1K, respectively) but the low-temperature spontaneous magnetization $M_s = 1.16\mu_B$/f.u. of URhGa is more than double the $M_s = 0.56\mu_B$/f.u. of UCoGa. The strongly reduced U moment in UCoGa is a clear indication of a much stronger delocalization of 5f-electrons compared to URhGa.

Such a situation can be intuitively expected when we consider the much smaller lattice parameters, particularly the $a$, in UCoGa with respect to URhGa. Consequently, the corresponding U-U and U-$T$ interatomic distances within the basal plane imply much larger 5f-5f and 5f-3d wave-function overlaps, with stronger 5f-ligand hybridization leading to much more delocalized 5f-electrons in UCoGa. From the point of view of TSFT, this situation is reflected in the significantly higher magnitude of the $T_C/T_0$ ratio (= 0.495) obtained for URhGa compared to the $T_C/T_0 = 0.182$ obtained for UCoGa. A higher $T_C/T_0$ ratio represents more localized magnetic electrons. Consistently with better localization of the 5f-electrons, the SF spectra for URhGa are much narrower both in energy and wave-vector space (smaller $T_0$ and $T_A$) than for UCoGa.

In Table 3.4 we can also see that the application of hydrostatic pressure on UCoGa and URhGa has a different effect on the corresponding values of $M_s$, $T_C$, and the TSFT parameters. With increasing applied pressure on UCoGa, $M_s$, $T_C$, and $T_C/T_0$ decrease rapidly. $T_0$ increases whereas $T_A$ almost does not change. On the other hand, $T_C$, $T_C/T_0$, and $T_A$ of URhGa slightly increase, while $M_s$ and $T_0$ remain invariant.

These results fit well with the general scenario of relations between electronic structure and magnetism in U compounds. URhGa appears in the conditions of moderate hybridization when a pressure-induced increase of hybridization increases the exchange of an interaction leading to an increase of $T_C$ without visible effect on $M_s$. On the contrary, UCoGa is in a strong hybridization mode, where a significant suppression of the U magnetic moments due to the increasing pressure prevails over the increased exchange integral, so that the $T_C$ and $T_C/T_0$ decrease rapidly with increasing pressure. From the point of view of TSFT, a decrease of $T_C/T_0$ means an increasing itinerancy of 5f-electrons, which leads to an extension of the SF spectrum indicated by an increasing $T_0$ value. These are the signatures

| $a$ [pm] | compound | $M_s$ [$\mu_B$/f.u.] | $F_1$ [K] | $T_A$ [K] | $T_0$ [K] | $T_C/T_0$ | $\frac{d \ln T_C}{dp}$ [GPa$^{-1}$] |
|---|---|---|---|---|---|---|---|
| 669.1 | $UCo_{0.98}Ru_{0.02}Al$ | 0.36 | 2311 | 1540 | 274 | 0.083 | -1.074 |
| 669.3 | UCoGa [93] | 0.56 | 3060 | 1750 | 267 | 0.182 | -0.09 |
| 695.8 | UIrAl [51, 21] | 0.96 | 820 | 861 | 241 | 0.257 | -0.005 |
| 697 | URhAl [21, 19, 99] | 1.05 | 428 | 340 | 64.5 | 0.365 | -0.003 |
| 700.6 | URhGa [93] | 1.17 | 741 | 480 | 83 | 0.495 | 0.037 |
| 701.7 | UPtAl [21] | 1.38 | 615 | 395 | 67.8 | 0.642 | 0.059 |

Table 3.5: Evolution of $a$ lattice parameter, ambient-pressure experimental values of $M_s$, calculated values of $F_1$, $T_A$, $T_A$, and $T_C/T_0$ from TSFT, and initial pressure coefficients $F_1$, $T_A$, $T_A$, and $T_C/T_0$ values for $p \to 0$ within a group of isostructural U$TX$ ferromagnets crystallizing in the hexagonal ZrNiAl-type structure. For full version of the table see A.9.

that URhGa gradually moves towards the strong 5f-ligand hybridization regime where the washout of U magnetic moments dominates due to increasing itinerancy of 5f-electrons so that $T_C$ and also $T_C/T_0$ will decrease in higher pressures.

In Table 3.5, UCoGa and URhGa are compared with several other isostructural U$TX$ ferromagnets for which the pressure effects are known. To facilitate further discussion also the lattice parameters are displayed. When inspecting Table 3.5 closely, one can observe a clear relation between the evolution of the lattice parameter $a$, the spontaneous magnetization $M_s$, the $T_C/T_0$ ratio, representing in TSFT the degree of 5f-electron localization, and the $\frac{dT_C}{dp}$ values. These parameters increase monotonously throughout Table 3.5. The increasing $a$ is directly associated with the proportionally increasing U-U and U-$T$ interatomic distances within the basal plane around which most of the 5f-5f overlaps and 5f-d hybridizations occur. Increasing localization of 5f-electrons can be expected when $a$ increases, which correlates with the increasing $T_C/T_0$ ratio. As to the sign of the initial pressure response of $T_C$, Table 3.5 has two parts: (a) URhAl and compounds above it with $\frac{d \ln T_C}{dp} < 0$ and (b) compounds with $\frac{d \ln T_C}{dp} > 0$ (URhGa, UPtAl). The limit $T_C/T_0$ value separating materials with positive to negative pressure response of $T_C$, respectively, can be roughly estimated as 0.43. The crossover of the change of $\frac{d \ln T_C}{dp}$ sign is located between URhAl and URhGa. The opposite signs of $\frac{dT_C}{dp}$ values observed for URhGa (positive) and URhAl (negative) demonstrate that the 5f-3p (URhAl) hybridization causes a stronger delocalization of the 5f-electrons than the 5f-4p (URhGa) hybridization. Let us shortly summarized the key properties of the discussed compounds.

**URhAl** shows an initial slight negative $\frac{dT_C}{dp}$. The rate of $T_C$ decrease accelerates with increasing pressure towards the loss of ferromagnetism observed at a tricritical point at 5.2 GPa [67] (similar to UCoGa, see Sec. 3.3.1).

**URhGa** investigation to higher pressures (see Sec. 3.3.2) revealed $T_C$ in URhGa increases linearly ($\frac{dT_C}{dp} \approx 1.1$K/GPa) whereas $\frac{dM_s}{dp}$ decreases with increasing pressure up to 4 GPa. In higher pressures, $\frac{dT_C}{dp}$ gradually decreases and the pressure, where $T_C$ reaches the maximum value, can be expected somewhere between 6 and 9 GPa. $M_s$ decreases much faster with increasing pressure above 4 GPa.

**UPtAl** also exhibits an increasing $T_C$ with increasing pressure [97, 100, 101]. $T_C$ reaches the maximum value at 6 GPa and then decreases with further increasing pressure up to 17 GPa, where the ferromagnetism is suppressed.

**UCoAl** deserves to be mentioned here, too, although it is not ferromagnetic at ambient conditions. Nevertheless, with increasing uniaxial stress applied on the UCoAl single crystal along the hexagonal c axis, a decrease of the critical field of metamagnetic transition is observed until it vanishes and a ferromagnetic ordering is established [102, 103]. On the other hand, the UCoAl crystal is compressed[2] along a; an increase in the critical field is observed [104, 105].

A detailed analysis (see A.9) shows counterexamples outside the ZrNiAl structure type — the opposite pressure response of URhGe and $UGe_2$ Curie temperatures with respect to expectations from the correlation between $T_C/T_0$ and $\frac{\mathrm{d}\ln T_C}{\mathrm{d}p}$ observed for the uniaxial $UTX$ ferromagnets adopting the hexagonal ZrNiAl-type structure indicates that the correlation is not a universal feature of U ferromagnets independent from the underlying crystal structure.

The reason may be connected with a more complex anisotropy of spin fluctuations in compounds with lower symmetries. The compression of the 5f-electron density towards the basal plane, together with strong spin-orbit coupling in the hexagonal $UTX$ compounds with the ZrNiAl-type structure, are the sources of huge uniaxial magnetocrystalline anisotropy with the easy-magnetization axis along the hexagonal $c$ axis. This makes the magnetism in these materials almost two-dimensional. The negligible magnetization observed in the basal plane (perpendicular to the $c$ axis) corroborates the idea that the transversal spin fluctuations are negligible [71] and the spin-fluctuation behavior is simplified. The complex magnetocrystalline anisotropy in the orthorhombic $UTX$ compounds and $UGe_2$ with different components along the main crystallographic directions together with the anisotropy of compressibility [106] and thermal expansion [107, 108, 109] probably does not allow us to apply the model applicable to the hexagonal $UTX$ compounds on these materials.

[2]It should be noted that this a-axis stress experiments in the hexagonal UCoAl crystal cannot bring definitive results with respect to this topic. A basal-plane stress experiment, in which the basal plane of the UCoAl crystal is uniformly stressed in all directions, whereas the crystal is free to dilate within the c-axis direction, is desirable for affecting the 5f-5f overlaps and 5f-d hybridizations around the plane.

# Conclusion

The project proposal, part of which outcomes are discussed in this Thesis, was originally aimed at the investigation of particular thermodynamic phenomena in the presumably well-known groups of compounds.

The most fruitful group of compounds was the U$TX$ system, where we were able to reach our original goal (investigate the temperature – magnetic field – pressure phase diagram, and the relation between purity and the features of this particular type of phase diagram). During this study, our attention was also brought to previously unknown features of the underlying physics of the U$TX$ group of compounds and the improvement (or, more precisely, improvement of understanding) of the preparation technology.

In particular, we were able to follow the phase separation in $UCo_{0.995}Ru_{0.005}Al$ and loss of magnetism with the hydrostatic pressure of $UCo_{0.990}Ru_{0.010}Al$. In the latter case, the electrical resistivity exponent $n$ changes from 2 (Fermi liquid-like) in the pure ferromagnetic state to $3/2$ in the paramagnetic ground state with increasing pressure. Although it has been shown that the doped system under high pressure shows the same magnetic ground state as pure UCoAl at ambient pressure, the subtle differences in the microscopic nature are reflected by a different power law, as the pure UCoAl follows $n = 5/3$.

Additionally, we investigated the universality classes in the studied compounds, leading to the observation of the change from 2D Ising to 3D Ising universality class happening when the 5f electrons become considerably itinerant due to reducing the $a$ lattice parameter.

We also put forward a proposition possibly leading to the explanation of the long-time singular behavior of the UPTAl compound, being (originally) the only one in the U$TX$ family of the compounds with the ZrNiAl structure following the initial increase of the Curie temperature with increasing hydrostatic pressure. Our novel investigation of the URhGa compound with similar behavior, and others following the general rule, leads us to propose a connection between the character of the spin fluctuation spectra and the pressure evolution of the $T_C$.

# Bibliography


[1] Benjamin A. Frandsen, Lian Liu, Sky C. Cheung, Zurab Guguchia, Rustem Khasanov, Elvezio Morenzoni, Timothy J.S. Munsie, Alannah M. Hallas, Murray N. Wilson, Yipeng Cai, Graeme M. Luke, Bijuan Chen, Wenmin Li, Changqing Jin, Cui Ding, Shengli Guo, Fanlong Ning, Takashi U. Ito, Wataru Higemoto, Simon J.L. Billinge, Shoya Sakamoto, Atsushi Fujimori, Taito Murakami, Hiroshi Kageyama, Jose Antonio Alonso, Gabriel Kotliar, Masatoshi Imada, and Yasutomo J. Uemura. Volume-wise destruction of the antiferromagnetic Mott insulating state through quantum tuning. *Nature Communications*, 7(1):12519, nov 2016.

[2] Elias Lahoud, O. Nganba Meetei, K. B. Chaska, A. Kanigel, and Nandini Trivedi. Emergence of a novel pseudogap metallic state in a disordered 2D mott insulator. *Physical Review Letters*, 112(20):206402, may 2014.

[3] Nihar R. Pradhan, Amber McCreary, Daniel Rhodes, Zhengguang Lu, Simin Feng, Efstratios Manousakis, Dmitry Smirnov, Raju Namburu, Madan Dubey, Angela R. Hight Walker, Humberto Terrones, Mauricio Terrones, Vladimir Dobrosavljevic, and Luis Balicas. Metal to Insulator Quantum-Phase Transition in Few-Layered ReS2. *Nano Letters*, 15(12):8377–8384, dec 2015.

[4] R. Schneider, A. G. Zaitsev, D. Fuchs, and H. V. Löhneysen. Superconductor-insulator quantum phase transition in disordered FeSe thin films. *Physical Review Letters*, 108(25):257003, jun 2012.

[5] M. Brando, D. Belitz, F. M. Grosche, and T. R. Kirkpatrick. Metallic quantum ferromagnets. *Reviews of Modern Physics*, 88(2):025006, may 2016.

[6] Hilbert V. Löhneysen, Achim Rosch, Matthias Vojta, and Peter Wölfle. Fermi-liquid instabilities at magnetic quantum phase transitions. *Reviews of Modern Physics*, 79(3):1015–1075, aug 2007.

[7] Y. Tokiwa, J. J. Ishikawa, S. Nakatsuji, and P. Gegenwart. Quantum criticality in a metallic spin liquid. *Nature Materials*, 13(4):356–359, apr 2014.

[8] S. E. Rowley, L. J. Spalek, R. P. Smith, M. P.M. Dean, M. Itoh, J. F. Scott, G. G. Lonzarich, and S. S. Saxena. Ferroelectric quantum criticality. *Nature Physics*, 10(5):367–372, may 2014.

[9] C. Pfleiderer, S. R. Julian, and G. G. Lonzarich. Non-Fermi-liquid nature of the normal state of itinerant-electron ferromagnets. *Nature*, 414(6862):427–430, nov 2001.

[10] D. Belitz, T. R. Kirkpatrick, and Jörg Rollbühler. Tricritical behavior in itinerant quantum ferromagnets. *Physical Review Letters*, 94(24):247205, jun 2005.

[11] D. Belitz and T. R. Kirkpatrick. First order transitions and multicritical points in weak itinerant ferromagnets. *Physical Review Letters*, 82(23):4707–4710, jun 1999.

[12] Thomas Andrews. XVIII. The Bakerian Lecture .—On the continuity of the gaseous and liquid states of matter . *Philosophical Transactions of the Royal Society of London*, 159:575–590, dec 1869.

[13] Leo P. Kadanoff. Scaling laws for ising models near Tc. *Physics Physique Fizika Physics Physique*, 2(6):263–272, jun 1966.

[14] Kenneth G. Wilson. Renormalization group and critical phenomena. I. Renormalization group and the Kadanoff scaling picture. *Physical Review B*, 4(9):3174–3183, nov 1971.

[15] Kenneth G. Wilson. Renormalization group and critical phenomena. II. Phase-space cell analysis of critical behavior. *Physical Review B*, 4(9):3184–3205, nov 1971.

[16] Kenneth G. Wilson. The renormalization group: Critical phenomena and the Kondo problem. *Reviews of Modern Physics*, 47(4):773–840, oct 1975.

[17] V. Sechovsky and L. Havela. Chapter 1 Magnetism of ternary intermetallic compounds of uranium. *Handbook of Magnetic Materials*, 11:1–289, 1998.

[18] K. Karube, T. Hattori, S. Kitagawa, K. Ishida, N. Kimura, and T. Komatsubara. Universality and critical behavior at the critical endpoint in the itinerant-electron metamagnet UCoAl. *Physical Review B - Condensed Matter and Materials Physics*, 86(2):024428, jul 2012.

[19] Naoyuki Tateiwa, Jiří Pospíšil, Yoshinori Haga, and Etsuji Yamamoto. Critical behavior of magnetization in URhAl: Quasi-two-dimensional Ising system with long-range interactions. *Physical Review B*, 97(6):064423, feb 2018.

[20] Vladimír Sechovský, Ladislav Havela, L Neuzil, Alexander V. Andreev, G. Hilscher, and C. Schmitzer. On the magnetic behaviour of some UTX compounds (X=Al, Ga, Sn; T=transition metal). *Journal of the Less-Common Metals*, 121:169 – 174, 1986.

[21] Naoyuki Tateiwa, Jiří Pospíšil, Yoshinori Haga, Hironori Sakai, Tatsuma D. Matsuda, and Etsuji Yamamoto. Itinerant ferromagnetism in actinide 5f -electron systems: Phenomenological analysis with spin fluctuation theory. *Physical Review B*, 96(3):035125, jul 2017.

[22] P. Javorsky, J. Schweizer, F. Givord, J. Boucherle, V. Sechovsky, A. Andreev, E. Lelievre-Berna, and F. Bourdarot. Uranium Form Factors in Selected UTX Compounds. *Acta Physica Polonica B*, 34(2):1425, feb 2003.

[23] Alexander V. Andreev, O. Chernyavski, Vladimír Sechovský, and V I Krylov. Influence of 3d-metal doping on magnetism of UNiGa. *Journal of Alloys and Compounds*, 353(1-2):102–106, apr 2003.

[24] K. Prokeš, V. Sechovský, A. Gukasov, A. V. Andreev, and H. Nakotte. Direct measurement of the magnetic anisotropy in UCoGa using polarized neutrons. *Physica B: Condensed Matter*, 276-278:564–565, 2000.

[25] A. Purwanto, R. A. Robinson, K. Prokeš, H. Nakotte, F. R. De Boer, L. Havela, V. Sechovský, N. C. Tuan, Y. Kergadallan, J. C. Spirlet, and J. Rebizant. Structure, transport and thermal properties of UCoGa. *Journal of Applied Physics*, 76(10):7040–7042, 1994.

[26] Petr Opletal, Petr Proschek, Barbora Vondráčková, David Aurélio, Vladimír Sechovský, and Jan Prokleška. Effect of thermal history on magnetism in UCoGa. *Journal of Magnetism and Magnetic Materials*, 490, 2019.

[27] A V Andreev, A V Deryagin, and R Y Yumaguzhin. Crystal structure and magnetic properties of UGaCo and UGaNi single crystals. *Soviet Physics - JETP*, 59(5):1082–1086, 1984.

[28] H. Nakotte, F. R. De Boer, L. Havela, P. Svoboda, V. Sechovský, Y. Kergadallan, J. C. Spirlet, and J. Rebizant. Magnetic anisotropy of UCoGa. *Journal of Applied Physics*, 73(10):6554–6556, 1993.

[29] A. V. Andreev, L. Havela, V. Sechovsky, M. I. Bartashevich, J. Šebek, R. V. Dremov, and I. K. Kozlovskaya. Ferromagnetism in the UCo1-xRuxAl quasiternary intermetallics. *Philosophical Magazine B: Physics of Condensed Matter; Statistical Mechanics, Electronic, Optical and Magnetic Properties*, 75(6):827–844, jun 1997.

[30] Petr Opletal. Critical behaviour in magnetic phase diagrams of uranium compounds, 2015.

[31] Michal Vališka, Petr Opletal, Jiří Pospíšil, Jan Prokleška, and Vladimír Sechovský. Evolution of magnetism in UCoGe and UCoAl with Ru doping. *Advances in Natural Sciences: Nanoscience and Nanotechnology*, 6(1):015017, jan 2015.

[32] A. V. Andreev, N. V. Mushnikov, T. Goto, and V. Sechovský. Alloying and pressure-induced transitions between 5f-band metamagnetism and ferromagnetism. *Physical Review B - Condensed Matter and Materials Physics*, 60(2):1122–1126, 1999.

[33] A. V. Andreyev and M. I. Bartashevich. New Group of Uranium Magnets. *Physics of Metals and Metallography*, 62(2):50–53, 1986.

[34] V. Sechovsky, L. Havela, P. Nozar, E. Brück, F. R. de Boer, A. A. Menovsky, K. H.J. Buschow, and A. V. Andreev. 5f-ligand hybridization and magnetism in UTX compounds. *Physica B: Physics of Condensed Matter*, 163(1-3):103–106, apr 1990.

[35] V. Sechovsky, L. Havela, F. R. de Boer, P. A. Veenhuizen, K. Sugiyama, T. Kuroda, E. Sugiura, M. Ono, M. Date, and A. Yamagishi. Hybridization and magnetism in U(Ru, Rh)X, X=Al, Ga. *Physica B: Physics of Condensed Matter*, 177(1-4):164–168, mar 1992.

[36] Alexander V. Andreev, Yoshinobu Shiokawa, Michihisa Tomida, Yoshiya Homma, Vladimir Sechovský, Nikolai V. Mushnikov, and Tsuneaki Goto. Magnetic Properties of a UPtAl Single Crystal. *Journal of the Physical Society of Japan*, 68(7):2426–2432, jul 1999.

[37] A. V. Andreev. Magnetization study of a UIrAl single crystal. *Journal of Alloys and Compounds*, 336(1-2):77–80, apr 2002.

[38] Noriaki Kimura, Rikio Settai, Yoshichika Ōnuki, Yoshichika Ōnuki, Etsuji Yamamoto, Hiroyuki Toshima, Kunihiko Maezawa, Haruyoshi Aoki, and Hisatomo Harima. Magnetoresistance and de Haas-van Alphen Effect in UPt3. *Journal of the Physical Society of Japan*, 64(10):3881–3889, oct 1995.

[39] E. Yamamoto, Y. Haga, T. D. Matsuda, S. Ikeda, Y. Inada, R. Settai, and Y. Onuki. High-quality single crystal growth of UGe2 and URhGe. *Journal of Magnetism and Magnetic Materials*, 272-276(SUPPL. 1):E171–E172, may 2004.

[40] Tatsuma D. Matsuda, Dai Aoki, Shugo Ikeda, Eetsuji Yamamoto, Yoshinori Haga, Hitoshi Ohkuni, Rikio Settai, and Yoshichika Onuki. Super clean sample of URu2Si2. *Journal of the Physical Society of Japan*, 77(SUPPL.A):362–364, jan 2008.

[41] Jiří Pospíšil, Karel Prokeš, Manfred Reehuis, Michael Tovar, Jana Poltierová Vejpravová, Prokleška Jan, and Vladimír Sechovský. Influence of sample preparation technology and treatment on magnetism and superconductivity of UCoGe. *Journal of the Physical Society of Japan*, 80(8):084709, aug 2011.

[42] N. T. Huy, Y. K. Huang, and A. de Visser. Effect of annealing on the magnetic and superconducting properties of single-crystalline UCoGe. *Journal of Magnetism and Magnetic Materials*, 321(17):2691–2693, sep 2009.

[43] E Yamamoto, Y Haga, T D Matsuda, Y Inada, R Settai, Y Tokiwa, and Y Onuki. SINGLE CRYSTAL GROWTH AND ANNEALING TEMPERATURE OF FERROMAGNETIC URhGe. *Acta Physica Polonica B*, 34(2):1059, 2003.

[44] A. Raghunathan, Y. Melikhov, J. E. Snyder, and D. C. Jiles. Theoretical model of temperature dependence of hysteresis based on mean field theory. *IEEE Transactions on Magnetics*, 46(6):1507–1510, jun 2010.

[45] David Jiles. *Introduction to Magnetism and Magnetic Materials*. CRC Press, sep 2015.

[46] H. R. Hilzinger and H. Kronmüller. Statistical theory of the pinning of Bloch walls by randomly distributed defects. *Journal of Magnetism and Magnetic Materials*, 2(1-3):11–17, dec 1975.

[47] Tristan Combier. *Ferromagnetic quantum criticality in the uranium-based ternary compounds URhSi, URhAl, and UCoAl*. PhD thesis, Université de Grenoble, 2014.

[48] N. Kimura, N. Kabeya, H. Aoki, K. Ohyama, M. Maeda, H. Fujii, M. Kogure, T. Asai, T. Komatsubara, T. Yamamura, and I. Satoh. Quantum critical point and unusual phase diagram in the itinerant-electron metamagnet UCoAl. *Physical Review B - Condensed Matter and Materials Physics*, 92(3):035106, jul 2015.

[49] Petr Opletal, Jan Prokleška, Jaroslav Valenta, Petr Proschek, Vladimír Tkáč, Róbert Tarasenko, Marie Běhounková, Šárka Matoušková, Mohsen M. Abd-Elmeguid, and Vladimír Sechovský. Quantum ferromagnet in the proximity of the tricritical point. *npj Quantum Materials*, 2(1):29, dec 2017.

[50] L. Jirman, V. Sechovský, L. Havela, W. Ye, T. Takabatake, H. Fujii, T. Suzuki, T. Fujita, E. Brück, and F. R. De Boer. Magnetic and transport properties of UNiGa. *Journal of Magnetism and Magnetic Materials*, 104-107(PART 1):19–20, feb 1992.

[51] A. V. Andreev, N. V. Mushnikov, F. Honda, V. Sechovský, P. Javorský, and T. Goto. Magnetic, magnetoelastic and other electronic properties of a UIrAl single crystal. *Journal of Magnetism and Magnetic Materials*, 272-276(SUPPL. 1):E337–E339, may 2004.

[52] Bernard Barbara, Christian BÉCle, Remy Lemaire, and D. P. Dominique Paccard. High-Performance Magnets of Rare-Earth Intermetallics Due to an Unusual Magnetization Process. *IEEE Transactions on Magnetics*, 7(3):654–656, 1971.

[53] Jan J. Van Den Broek and Hinne Zijlstra. Calculation of Intrinsic Coercivity of Magnetic Domain Walls in Perfect Crystals. *IEEE Transactions on Magnetics*, 7(2):226–230, 1971.

[54] A. Deryagin and A. Andreev. Magnetic properties, and the crystal and domain structures of the uranium intermetallic compound UCo5.3. *Soviet Journal of Experimental and Theoretical Physics*, 44:610, 1976.

[55] J. J. Wysłocki, W. Suski, and A. Baran. Magnetic domain structures, domain wall energies and magnetization processes in UFe10Si2 and UCo10Si2 intermetallic compounds. *Journal of The Less-Common Metals*, 163(1):115–121, 1990.

[56] Xinzhou Tan, Morgann Berg, Alex De Lozanne, Jeehoon Kim, R. E. Baumbach, E. D. Bauer, J. D. Thompson, and F. Ronning. Imaging the magnetic states in an actinide ferromagnet UMn2Ge2. *Physical Review Materials*, 2(7), 2018.

[57] David S. Parker, Nirmal Ghimire, John Singleton, J. D. Thompson, Eric D. Bauer, Ryan Baumbach, David Mandrus, Ling Li, and David J. Singh. Magnetocrystalline anisotropy in UMn2Ge2 and related Mn-based actinide ferromagnets. *Physical Review B - Condensed Matter and Materials Physics*, 91(17), 2015.

[58] Alex Hubert and Rudolf Schäfer. *Magnetic Domains*. Springer Berlin Heidelberg, Berlin, Heidelberg, 1998.

[59] D. Płusa, R. Pfranger, and B. Wysłocki. Dependence of domain width on crystal thickness in YCo5 single crystals. *Physica Status Solidi (a)*, 92(2):533–538, 1985.

[60] R. Bodenberger and A. Hubert. Zur bestimmung der blochwandenergie von einachsigen ferromagneten. *Physica Status Solidi (a)*, 44(1):K7–K11, 1977.

[61] Stephen Blundell. Oxford master series in condensed matter physics, 2001.

[62] L Havela, M. Diviš, V. Sechovský, A.V. Andreev, F. Honda, G. Oomi, Y. Méresse, and S. Heathman. U ternaries with ZrNiAl structure — lattice properties. *Journal of Alloys and Compounds*, 322(1-2):7–13, jun 2001.

[63] Petr Opletal, Vladimír Sechovský, and Jan Prokleška. Different universality classes of isostructural U TX compounds (T= Rh, Co, Co0.98Ru0.02; X= Ga, Al). *Physical Review B*, 102(22):224438, dec 2020.

[64] I Syozi. Statistics of [the] kagomé lattice. *Prog. Theor. Phys.*, 6:306–308, 1951.

[65] F. Honda, T. Eto, G. Oomi, A. V. Andreev, V. Sechovský, N. Takeshita, and N. Môri. Collapse of 5f-electron ferromagnetism in UPtAl under high pressures. *High Pressure Research*, 22(1):159–162, jan 2002.

[66] Masahiko Hatatani and Tôru Moriya. Ferromagnetic Spin Fluctuations in Two-Dimensional Metals. *Journal of the Physical Society of Japan*, 64(9):3434–3441, sep 1995.

[67] Yusei Shimizu, Daniel Braithwaite, Bernard Salce, Tristan Combier, Dai Aoki, Eduardo N. Hering, Scheilla M. Ramos, and Jacques Flouquet. Unusual strong spin-fluctuation effects around the critical pressure of the itinerant Ising-type ferromagnet URhAl. *Physical Review B - Condensed Matter and Materials Physics*, 91(12):125115, mar 2015.

[68] A. V. Kolomiets, L. Havela, V. Sechovský, L. E. DeLong, D. B. Watkins, and A. V. Andreev. Evidence for an extended critical region near the metamagnetic transition of UCoAl. *Journal of Applied Physics*, 83(11):6435–6437, jun 1998.

[69] Dai Aoki, Tristan Combier, Valentin Taufour, Tatsuma D. Matsuda, Georg Knebel, Hisashi Kotegawa, and Jacques Flouquet. Ferromagnetic quantum critical endpoint in UCoAl. *Journal of the Physical Society of Japan*, 80(9):094711, sep 2011.

[70] Y. Sang, D. Belitz, and T. R. Kirkpatrick. Disorder dependence of the ferromagnetic quantum phase transition. *Physical Review Letters*, 113(20):1–5, 2014.

[71] N. V. Mushnikov, T. Goto, K. Kamishima, H. Yamada, A. V. Andreev, Y. Shiokawa, A. Iwao, and V. Sechovsky. Magnetic properties of the 5f itinerant electron metamagnet ucoal under high pressure. *Physical Review B - Condensed Matter and Materials Physics*, 59(10):6877–6885, mar 1999.

[72] A. V. Andreev, M. I. Bartashevich, T. Goto, K. Kamishima, L. Havela, and V. Sechovský. Effects of external pressure on the 5f-band metamagnetism in UCoAl. *Physical Review B*, 55(9):5847–5850, mar 1997.

[73] Dai Aoki, Andrew Huxley, Eric Ressouche, Daniel Braithwaite, Jacques Flouquet, Jean Pascal Brison, Elsa Lhotel, and Carley Paulsen. Coexistence of superconductivity and ferromagnetism in URhRe. *Nature*, 413(6856):613–616, oct 2001.

[74] N. T. Huy, A. Gasparini, D. E. De Nijs, Y. Huang, J. C.P. Klaasse, T. Gortenmulder, A. De Visser, A. Hamann, T. Görlach, and H. V. Löhneysen. Superconductivity on the border of weak itinerant ferromagnetism in UCoGe. *Physical Review Letters*, 99(6):067006, aug 2007.

[75] H. Yamada. Metamagnetic transition and susceptibility maximum in an itinerant-electron system. *Physical Review B*, 47(17):11211–11219, may 1993.

[76] L. Havela, A. Kolomiets, F. Honda, A. V. Andreev, V. Sechovsky, L. E. DeLong, Y. Shiokawa, T. Kagayama, and G. Oomi. Stability of the non-Fermi liquid state in UCoAl. *Physica B: Condensed Matter*, 281-282:379–380, jun 2000.

[77] T. R. Kirkpatrick and D. Belitz. Stable phase separation and heterogeneity away from the coexistence curve. *Physical Review B*, 93(14):144203, apr 2016.

[78] R. P. Smith, M. Sutherland, G. G. Lonzarich, S. S. Saxena, N. Kimura, S. Takashima, M. Nohara, and H. Takagi. Marginal breakdown of the Fermi-liquid state on the border of metallic ferromagnetism. *Nature*, 455(7217):1220–1223, oct 2008.

[79] T. R. Kirkpatrick and D. Belitz. Universal low-temperature tricritical point in metallic ferromagnets and ferrimagnets. *Physical Review B - Condensed Matter and Materials Physics*, 85(13):134451, apr 2012.

[80] V Sechovsky, F Honda, K Prokes, O Syshchenko, A V Andreev, and J Kamarad. Pressure-induced phenomena in U intermetallics. *Acta Phys. Pol. B*, 34:1377–1386, 2003.

[81] V Sechovský, L Havela, N Pillmayr, G Hilscher, and A V Andreev. On the magnetic behaviour of UGaT series. *Journal of Magnetism and Magnetic Materials*, 63-64(C):199–201, 1987.

[82] A Arrott. Criterion for ferromagnetism from observations of magnetic isotherms. *Physical Review*, 108(6):1394–1396, 1957.

[83] A Arrott and J E Noakes. Approximate equation of state for nickel near its critical temperature. *Physical Review Letters*, 19(14):786–789, 1967.

[84] J S Kouvel and M E Fisher. Detailed magnetic behavior of nickel near its curie point. *Physical Review*, 136(6A):A1626–A1632, 1964.

[85] V Privman, P C Hohenberg, and A Aharony. Universal Critical-Point Amplitude Relations. *Phase Transitions and Critical Phenomena*, 14:1–134, 1991.

[86] B. Widow. Equation of state in the neighborhood of the critical point. *The Journal of Chemical Physics*, 43(11):3898–3905, dec 1965.

[87] M E Fisher, S.-K. Ma, and B G Nickel. Critical exponents for long-range interactions. *Physical Review Letters*, 29(14):917–920, 1972.

[88] T Takahashi, N Sato, T Yokoya, A Chainani, T Morimoto, and T Komatsubara. Dual Character of 5f Electrons in UPd2Al3 Observed by High-Resolution Photoemission Spectroscopy. *Journal of the Physical Society of Japan*, 65(1):156–159, 1996.

[89] G Zwicknagl. 5f Electron correlations and core level photoelectron spectra of Uranium compounds. *Physica Status Solidi (B) Basic Research*, 250(3):634–637, 2013.

[90] G Zwicknagl. 3 = 2+1: Partial localization, the dual character of 5f electrons and heavy fermions in U compounds. *Journal of Magnetism and Magnetic Materials*, 272-276(SUPPL. 1):e119–e120, 2004.

[91] P Rhodes and E P Wohlfarth. The effective Curie-Weiss con-stant of ferromagnetic metals and alloys. *Proc. R. Soc. London*, 273(1353), 1963.

[92] E P Wohlfarth. Magnetic properties of crystallineand amorphous alloys: A systematic discussion based on the Rhodes-Wohlfarth plot. *Journal of Magnetism and Magnetic Materials*, 7(1-4):113–120, 1978.

[93] A. E. Dwight. Alloy Chemistry of Thorium, Uranium, and Plutonium Compounds. In *Developments in the Structural Chemistry of Alloy Phases*, pages 181–226. Springer US, Boston, MA, 1969.

[94] D J Lam, J B Darby Jr., J W Downey, and L J Norton. Equiatomic ternary compounds of uranium and aluminium with group viii transition elements. *Journal of Nuclear Materials*, 22(1):22–27, 1967.

[95] Y Takahashi. Spin-fluctuation theory of quasi-two-dimensional itinerant-electron ferromagnets. *Journal of Physics Condensed Matter*, 9(47):10359–10372, 1997.

[96] P A Veenhuizen, F R De Boer, A A Menovsky, V Sechovsky, and L Havela. P.A. Veenhuizen, F.R. de Boer, A.A. Menovsky, V. Sechovsky, L. Havela, MAGNETIC-PROPERTIES OF URuAl and URhAl SINGLE-CRYSTALS. *J. de Phys.*, 49:C8–485, 1988.

[97] V. Sechovský, F. Honda, K. Prokeš, J. C. Griveau, A. V. Andreev, Z. Arnold, J. Kamarád, and G. Oomi. Pressure effects on magnetism in U intermetallics: The UPtAl case. *Journal of Magnetism and Magnetic Materials*, 290-291 PA:629–632, apr 2005.

[98] Yoshinori Takahashi. *Spin Fluctuation Theory of Itinerant Electron Magnetism*, volume 253 of *Springer Tracts in Modern Physics*. Springer Berlin Heidelberg, Berlin, Heidelberg, 2013.

[99] Tristan Combier, Dai Aoki, Georg Knebel, and Jacques Flouquet. Ferromagnetic quantum criticality studied by hall effect measurements in UCoAl. *Journal of the Physical Society of Japan*, 82(10):104705, 2013.

[100] A.V. Andreev, J. Kamarád, F. Honda, G. Oomi, V. Sechovský, and Y. Shiokawa. Magnetoelasticity of UPtAl. *Journal of Alloys and Compounds*, 314(1-2):51–55, jan 2001.

[101] A. Andreev, M. Diviš, P. Javorský, K. Prokeš, V. Sechovský, J. Kuneš, and Y. Shiokawa. Electronic structure and magnetism in UPtAl. *Physical Review B*, 64(14):144408, sep 2001.

[102] Y. Ishii, M. Kosaka, Y. Uwatoko, A. V. Andreev, and V. Sechovský. Ferromagnetism induced in UCoAl under uniaxial pressure. *Physica B: Condensed Matter*, 334(1-2):160–166, jun 2003.

[103] Yusei Shimizu, Bernard Salce, Tristan Combier, Dai Aoki, and Jacques Flouquet. Uniaxial-stress-induced ferromagnetism in the itinerant metamagnetic compound UCoAl probed by magnetostriction measurements. *Journal of the Physical Society of Japan*, 84(2):2–5, 2015.

[104] Shanta R. Saha, Hitoshi Sugawara, Yuji Aoki, Hideyuki Sato, Tatsuma D. Matsuda, Yoshinori Haga, Etsuji Yamamoto, and Yoshichika Onuki. Transport properties in UCoAl under uniaxial pressure. *Physica B: Condensed Matter*, 329-333(II):530–531, may 2003.

[105] Kosuke Karube, Shunsaku Kitagawa, Taisuke Hattori, Kenji Ishida, Noriaki Kimura, and Takemi Komatsubara. Anisotropic uniaxial pressure response in UCoAl studied by nuclear magnetic resonance measurement. *Journal of the Physical Society of Japan*, 83(8):084706, 2014.

[106] A. M. Adamska, L. Havela, S. Surble, S. Heathman, J. Pospísil, and S. Danis. Pressure effect on the crystal lattice of unconventional superconductor UCoGe. *Journal of Physics Condensed Matter*, 22(27):275603, jul 2010.

[107] Dai Aoki, Frédéric Hardy, Atsushi Miyake, Valentin Taufour, Tatsuma D. Matsuda, and Jacques Flouquet. Properties of ferromagnetic superconductors. *Comptes Rendus Physique*, 12(5-6):573–583, jun 2011.

[108] A. Gasparini, Y. K. Huang, N. T. Huy, J. C.P. Klaasse, T. Naka, E. Slooten, and A. De Visser. The superconducting ferromagnet UCoGe. *Journal of Low Temperature Physics*, 161(1-2):134–147, jun 2010.

[109] F. Hardy, C. Meingast, V. Taufour, J. Flouquet, H. V. Löhneysen, R. A. Fisher, N. E. Phillips, A. Huxley, and J. C. Lashley. Two magnetic grüneisen parameters in the ferromagnetic superconductor UGe2. *Physical Review B - Condensed Matter and Materials Physics*, 80(17):174521, nov 2009.

# A. Related papers

# A.1

Vališka, M., Opletal, P., Pospíšil, J., Prokleška, J., Sechovsky, V. (2015). Evolution of magnetism in UCoGe and UCoAl with Ru doping. Advances in Natural Sciences: Nanoscience and Nanotechnology,6(1),015017,doi:10.1088/2043-6262/6/1/015017

# A.2

Opletal, P., Proschek, P., Vondráčková, B., Aurélio, D., Sechovský, V., Prokleška, J. (2019). Effect of thermal history on magnetism in UCoGa. Journal of Magnetism and Magnetic Materials, 490, 165464,doi:10.1016/j.jmmm.2019.165464

# A.3

Opletal, P., Uhlířová, K., Kalabis, I., Sechovský, V., Prokleška, J. (2020). Extreme narrow magnetic domain walls in U ferromagnets: The UCoGa case. Materials Today Communications, 24, 101017,doi:0.1016/j.mtcomm.2020.101017

# A.4

Míšek, M., Prokleška, J., Opletal, P., Proschek, P., Kaštil, J., Kamarád, J., Sechovský, V. (2017). Pressure-induced quantum phase transition in the itinerant ferromagnet UCoGa. AIP Advances, 7(5), 055712,doi:10.1063/1.4976300

# A.5

Míšek, M., Proschek, P., Opletal, P., Sechovský, V., Kaštil, J., Kamarád, J., Žáček, M., Prokleška, J. (2018). Pressure evolution of magnetism in URhGa. AIP Advances, 8(10), 101316,10.1063/1.5043134

# A.6

Opletal, P., Prokleška, J., Valenta, J., Proschek, P., Tkáč, V., Tarasenko, R., Běhounková, M., Matoušková, Š., Abd-Elmeguid, M. M., Sechovský, V. (2017). Quantum ferromagnet in the proximity of the tricritical point. Npj Quantum Materials, 2(1),doi:10.1038/s41535-017-0035-6

# A.7

Opletal, P., Prokleška, J., Valenta, J., Sechovský, V. (2018). Electrical resistivity across the tricriticality in itinerant ferromagnet. AIP Advances, 8(5), 055710,doi:10.1063/1.5007692

# A.8

Opletal, P., Sechovský, V., Prokleška, J. (2020). Different universality classes of isostructural U$TX$ compounds ($T$=Rh, Co, $Co_{0.98}Ru_{0.02}$; $X$=Ga,Al). Physical Review B, 102(22),doi:10.1103/PhysRevB.102.224438

# A.9

Opletal, P., Valenta, J., Proschek, P., Sechovský, V., Prokleška, J. (2020). Effect of localization of 5f -electrons and pressure on magnetism in uranium intermetallics in spin-fluctuation theory. Physical Review B, 102(9), doi:10.1103/PhysRevB.102.094409